MASTERARBEIT | MASTER'S THESIS

Titel | Title

Effects of surface water donation on groundwater dynamics and ecology in the Upper Lobau

verfasst von | submitted by

Sarah Steitzinger BEd

angestrebter akademischer Grad | in partial fulfilment of the requirements for the degree of

Master of Education (MEd)

Wien | Vienna, 2026

Studienkennzahl lt. Studienblatt | Degree programme code as it appears on the student record sheet:	UA 199 502 525 02
Studienrichtung lt. Studienblatt | Degree programme as it appears on the student record sheet:	Masterstudium Lehramt Sek (AB) Unterrichtsfach Biologie und Umweltbildung Unterrichtsfach Psychologie und Philosophie
Betreut von | Supervisor:	Univ.-Prof. Mag. Dr. Christian Griebler

Abstract

The Upper Lobau has experienced disconnection from the Danube due to the river regulation, leading to declining groundwater levels, altered water chemistry and habitat loss. To mitigate these impacts a surface water donation strategy was implemented, reconnecting former river branches via controlled inflows from the New Danube to restore hydrological connectivity and support wetland ecosystem functions. This thesis investigated the effects of surface water donation on groundwater levels, hydrochemistry, microbial activity, fauna abundance and composition at three groundwater wells from April 2023 to January 2025. Results demonstrated that surface water donation led to significant increases in groundwater levels at all wells. Other measurable effects of the donation were limited to the well LSMB, closest to the surface water. At this well, microbial activity increased significantly, hydrochemical composition and redox conditions changed and also groundwater fauna responded to the donation. In contrast, LSMI and LSMC exhibited stable hydrochemical conditions, no changes in microbial activity and no responses of groundwater fauna resulting to the donation. These findings indicate that surface water donation in this area induce localized hydrochemical and ecological changes in groundwater, with effects decreasing with distance from the recharge source.

Zusammenfassung

Die Obere Lobau wurde aufgrund der Flussregulierung von der Donau abgeschnitten, was zu sinkenden Grundwasserspiegeln, veränderter Hydrochemie und Habitatverlust führte. Um diese Auswirkungen zu minimieren, wurde eine Dotation mit Oberflächenwasser eingeführt, bei der ehememalige Gewässer über kontrollierte Wasserzufuhr der neuen Donau wieder mit Wasser versorgt werden, um die Funktion des Feuchtgebiets zu unterstützen. In dieser Arbeit wurden die Auswirkungen der Dotation auf Grundwasserspiegel, Hydrochemie, mikrobielle Aktivität und Fauna an drei Grundwasser Messstellen von April 2023 bis Januar 2025 untersucht. Die Ergebnisse zeigten, dass die Dotation zu einem signifikanten Anstieg der Grundwasserspiegel an allen untersuchten Messstellen führte. Andere messbare Effekte waren jedoch auf die Messstelle LSMB beschränkt, die dem Oberflächenwasser am nächsten liegt. In dieser Messsstelle stieg die mikrobielle Aktivität signifikant an, es traten Veränderungen hinsichtlich hydrochemischer und Redoxbedingungen auf und auch die Grundwasserfauna reagierte auf die Dotation. Im Gegensatz dazu zeigten LSMI und LSMC stabile hydrochemische Bedingungen, nur geringe Änderungen der mikrobiellen Aktivität und keine Reaktion der Grundwasserfauna, die auf die Dotation zurückzuführen ist. Die Ergebnisse verdeutlichen, dass Oberflächenwasser Dotation in diesem Gebiet lokalisierte ökologische und biogeochemische Veränderungen im Grundwasser hervorrufen kann, deren Effekte mit zunehmender Entfernung vom Oberflächenwasser abnehmen.

Acknowledgements

I would like to thank my supervisor Univ.-Prof. Mag. Dr. Christian Griebler for the guidance and support throughout the entire thesis. Furthermore, I want to thank Gabriele Schwammel and Hubert Kraill for their help regarding preparation of the material for our fieldwork and support with lab analysis. I want to thank Dr. Grit Rasch for her help and introduction to ATP and TCC measurements. Moreover I want to express my gratitude to Dr. Dr. Santiago Gaviria-Melo who provided an identification key for stygofauna taxonomy. Special thanks to Dr. Clemens Karwautz and Angela Cukusic for providing a pipeline for statistical analyses.

We acknowledge the support from the Magistratsabteilung (MA) 31, who granted us access to the three groundwater wells in the Upper Lobau and associated informations. Thereby we want to thank Marija Zubanovic Pichler, Gerhard Vondra and Gabriele Bayer. Furthermore we express our gratitude to Sigrid Scheikl and Alexander Faltejsek from the MA 49. Moreover, we want to thank the Nationalpark Donauauen GmbH for their support and permission to do research in the national park, in detail Karoline Zsak and Christian Baumgartner.

A special thank you goes to my family and friends for always supporting and believing in me.

Content

1 Introduction 1
1.1. Hypotheses 4
2 Material and Methods 5
2.1. Sampling area 5
2.2. Sampling 7
2.3. Analysis 8
2.3.1. Determination of Adenosine Triphosphate (ATP) 8
2.3.2. Determination of Total Cell Counts (TCC) 9
2.3.3. Greenhouse gas measurement: Carbon Dioxide and Methane 9
2.3.4. Measurement of Dissolved organic carbon (DOC) and dissolved inorganic carbon (DIC) 10
2.3.5. Water chemistry 10
2.3.6. Fauna examination 11
2.3.7. Statistical data analysis 12
3 Results 14
3.1. Environmental parameters 14
3.1.1. Groundwater table 14
3.1.2. Electrical conductivity (EC) 15
3.1.3. Dissolved Oxygen (DO) 16
3.1.4. Temperature 17
3.1.5. pH 17
3.2. Major ions 19
3.3. Nutrients 21
3.3.1. Ammonium (NH_4^+) 21
3.3.2. Phosphate (PO_4^{3-}) 21
3.3.3. Total Phosphorus (P) 22
3.4. Redox sensitive parameters 24
3.4.1. Nitrate (NO_3^-) 24
3.4.2. Nitrite (NO_2^-) 24
3.4.3. Sulfate (SO_4^{2-}) 25
3.4.4. Sulfide (HS^-) 26
3.4.5. Iron (Fe^{2+}) 27
3.4.6. Manganese (Mn^{2+}) 28
3.5. Carbon species 29
3.5.1. Dissolved organic carbon (DOC) 29
3.5.2. Dissolved inorganic carbon (DIC) 29
3.6. Microbial abundance and activity 31

3.6.1. Total cell counts (TCC) ... 31
3.6.2. Microbial activity (intracellular ATP) ... 31
3.7. Greenhouse gases ... 32
3.7.1. Methane (CH_4) ... 32
3.7.2. Carbon dioxide (CO_2) ... 33
3.8. Fauna ... 35
3.8.1. Distribution and abundance of stygobiont, stygophile and stygoxene taxonomic groups ... 35
3.8.2. Absolute Abundance and taxonomic composition ... 36
3.8.3. Relative Abundance ... 39
3.8.4. Shannon Diversity ... 42
3.8.5. Taxa richness ... 43
3.9. Phase and site-specific correlation patterns during donation periods and periods without donation ... 45
4 Discussion ... 48
4.1. Groundwater level response to surface water donation ... 48
4.2. Effects of surface water donation at LSMB ... 49
4.3. Changes in Redox-sensitive correlation structures during surface water donation ... 51
4.4. Groundwater quality ... 53
4.5. Site specific groundwater conditions ... 54
4.6. Dynamics at LSMC ... 55
4.7. Fauna ... 55
4.8. Evaluation of the hypotheses ... 57
5 Conclusion ... 58
6 References ... 59
6.1. Internet sources ... 66
7 List of Figures ... 67
8 List of Tables ... 69
9 Appendix ... 70

1 Introduction

Wetlands are unique ecosystems that are permanently or seasonally flooded and occur worldwide (Teresa et al., 2024). They are characterized by the seasonal or constant presence of surface water, which interacts with groundwater facilitating the transport, deposition and remobilization of alluvial sediments and nutrients and the presence of special microclimates (Wittmann, 2022). Wetlands consist of interconnected elements such as shore vegetation, soil and water. As a result of flooding and soil saturation wetlands are a transition zone between terrestrial and aquatic habitats and have a great biodiversity (Ye et al., 2018). Due to their hydrological connection to other ecosystems wetlands are particularly vulnerable (Faulkner, 2004). Beside providing habitats for plant and animal species, wetlands fulfill several important functions, including water retention and purification, groundwater recharge and storage, nutrient cycling (Teresa et al., 2024), reducing the risk of floods (Opperman et al., 2024) and regulating local climate (Ye et al., 2018).

Unfortunately, humans have destroyed more than half of the world's wetlands through drainage, daming and structural changes of river hydromorphology and other activities (Mitsch, 2005). The decline in wetland health is further caused by changes in land use, extensive agriculture and the expansion of urban areas (Kundu et al., 2024, Faulkner, 2004), along with pollution and climate change (Kundu et al., 2024). Especially urban wetland areas decreased continously over the years. In comparison to natural wetlands, many urban wetlands are now characterized by artificial alterations, reduced biodiversity and severe water pollution (Ye et al., 2018). As a result of channel correction flow velocities increased, riverbeds eroded, groundwater exchange is reduced and the connection between floodplains and the river channel is weakened (Tena et al., 2020). All of these alterations led to more uneven distribution of wetlands, resulting in smaller, more isolated areas with limited connectivity between patches. This fragmentation has further instensified the disruption of wetland habitats (Ye et al., 2018). Water bodies with poorer connection to surface water experience greater habitat loss than those with better surface water connections. The limited water exchange due to disconnection from the main river, combined with prolonged drought conditions, further impairs the ecosystems by causing low oxygen levels (Coder et al., 2025). Reduced groundwater levels additionally modify the interaction between groundwater and surface water, strongly affecting ecology in wetland areas. Decreasing groundwater levels influence the overall water balance but also nutrient distribution and can deterioreate water quality in wetlands (Havril et al., 2018). Biodiversity forms the foundation of human survival and societal development, playing an essential role in shaping sustainable urban ecosystems. The rich variety of flora and fauna in these habitats enhances the stability and resilience of urban ecosystems (Ye et al., 2018). Losing wetlands also means losing the ability to provide clean water, prevent floods, maintain biological biodiversity (Mitsch, 2005) and the environmental water cycle (Teresa et al., 2024).

Preserving wetlands within urban areas comes with various difficulties, including reduced hydrological functions, changed water regimes by barriers, wastewater pollution and the degradation of habtitats and declining biodiversity due to the introduction of invasive species (Alikhani et al., 2021). Restoring or maintaining the connection between rivers and their floodplains is very important because of the wide range of ecological and social advantages. These include improving water quality, storing carbon and nutrients, recharging groundwater, reducing the risk of floods in areas where human depend on avoiding floods (Opperman et al., 2024) and offering habitats for various species. In addition the livability of cities is improved by urban wetlands, because they reduce urban heat islands and mitigate climate change impacts in general (Alikhani et al., 2021). Also the remaining floodplains are utilized for recreational purposes (Hein et al., 2006).

The Lobau, a floodplain wetland located on the eastern edge of the city of Vienna, covers an area of 23 hectares and represents 24% of the Donau-Auen National Park (IS1: Stadt Wien, a). It is a remaining fragment of what was once an extensive and dynamic floodplain region along the Danube's left bank. Due to the river regulation works of the nineteenth century, the area became disconnected from the main river channel, with the Schönauer Schlitz remaining as its only direct connection to the Danube (Weigelhofer et al., 2013), however, only during high water levels. The disconnection from the Danube during the river regulation in 1875, the hydropower plant Freudenau, combined with various forms of land use have contributed to declining groundwater levels and a large scale loss of aquatic habitats (Weigelhofer et al., 2005). The loss of aquatic habitats threatens the species diversity of aquatic flora and fauna, which would continue to decline without restoration measures (Baart et al., 2013). In addition, the dynamic water supply from the Danube, with its fluctuating water levels, which is essential for a floodplain landscape, is missing. The water level in the Lobau is now regulated mainly by groundwater. The expansion of hydropower plants have caused the deepening of the Danube's riverbed. This led to decreasing groundwater levels in the surrounding areas. This trend was also intensified by growing agricultural groundwater use in the Marchfeld (IS2: Stadt Wien b).

A strategy, known as surface water supply (donation) was proposed, involving a controlled reconnection of former river branches to the Danube. The purpose of this strategy is to preserve the condition of the Lobau as species-rich and ecologically valuable. The goal of the project was to significantly increase surface and groundwater levels and thereby supporting a diverse network of water bodies and wetland habitats (Weigelhofer et al.,2005). Since 2001 the Upper Lobau has been supplied with water from the New Danube and the Old Danube in order to protect the local water bodies from drying out (IS2: Stadt Wien b; Funk et al., 2009). A channel was constructed to connect the Old Danube with the Upper Lobau, along with controllable weirs between the New Danube and the Upper Lobau. These structures prevent flooding and mitigate potential negative impacts on drinking water. The water supply is also regulated by quality thresholds for dissolved organic carbon (DOC), coliform bacteria, total phosphorus, and chlorophyll-a to prevent contamination and eutrophication (Funk et al., 2009). During the vegetation period, up to 500 L/s, in case of availability, could be supplied from the New or Old Danube into the former river branch system between Mühlwasser and Groß Enzersdorfer Arm. Although actual inflows were on average below 300 L/s due to floods, stabilizing effects on water quality were already observed. Based on these positive results water supply to the Upper Lobau has been ongoing since 2005. The donation enhances water exchange, providing additional hydrological control over nutrient dynamics and improving water quality in the reconnected water bodies (Weigelhofer et al., 2005). Because the previous water supply is insufficient, the inflow to the water bodies of the Upper Lobau is improved through a new secondary water supply since 2023. Water from the New Danube is guided via an underground pipeline to the Panozzalacke and from there via the Fasangartenarm to other water bodies of the Upper Lobau (IS3: Stadt Wien c).

To investigate the effects of surface water donation in the Upper Lobau on groundwater, this thesis examines whether the surface water recharge leads to measurable changes in biological and hydrochemical conditions in groundwater, as well as in the abundance and composition of stygobiont fauna. Groundwater from three wells in the Upper Lobau was monitored from April 2023 to January 2025 to evaluate these effects.

1.1. Hypotheses

H1: Groundwater levels rise during periods of surface water donation and groundwater recharge.

H2: Surface water supply leads to improved groundwater quality in terms of dissolved oxygen.

H3: Dissolved organic carbon (DOC) concentrations in groundwater increase during donation periods, due to surface water infiltration.

H4: Surface water donation transports in microbes and stimulates microbial communities, resulting in higher adenosine triphosphate (ATP) and higher total cell counts (TCC) in groundwater.

H5: Abundance of fauna in the shallow aquifer and diversity is higher during donation periods.

H6: The influence of surface water donation on groundwater conditions decreases with distance from the surface water.

2 Material and Methods

2.1. Sampling area

The floodplain Lobau is located on the northern bank at the eastern city limits of Vienna (Baart et al., 2013), with a total area of about 20 km² (Weigelhofer et al., 2011). The area includes former active river channels, floodplain water bodies and young floodplain sections. In its original state the floodplain was braided and anabranching with high rates of morphological change and frequent habitat regeneration (Baart et al., 2013).

The Lobau consists of an upper and a lower part called the Upper Lobau and the Lower Lobau. The study area is in the Upper Lobau. The Upper Lobau is a 531 ha large former floodplain segment of the Danube (Funk et al., 2009; Weigelhofer et al., 2011), with about 27.5 ha of backwaters (Weigelhofer et al., 2011). It is now fully disconnected from floods and embedded in Vienna's settlement area and is therefore heavily influenced by human activity and intensively used as a recreation area for hiking, cycling and bathing (Preiner et al., 2018).

Three groundwater monitoring wells (LSMB, LSMI, and LSMC) were selected along a transect from the Fasangartenarm to the Markethäufel drinking water production well. They were regularly sampled, together with the oxbow lake Panozzalacke. Surface water from the Fasangartenarm was sampled when water was present during the donation periods. The well LSMB is situated closest to the surface water Fasangartenarm, LSMC is located close to the Markethäufel production well and represents the most distant sampling point from the Fasangartenarm, while LSMI lies between these two sampling sites (Figure 1; Table 1).

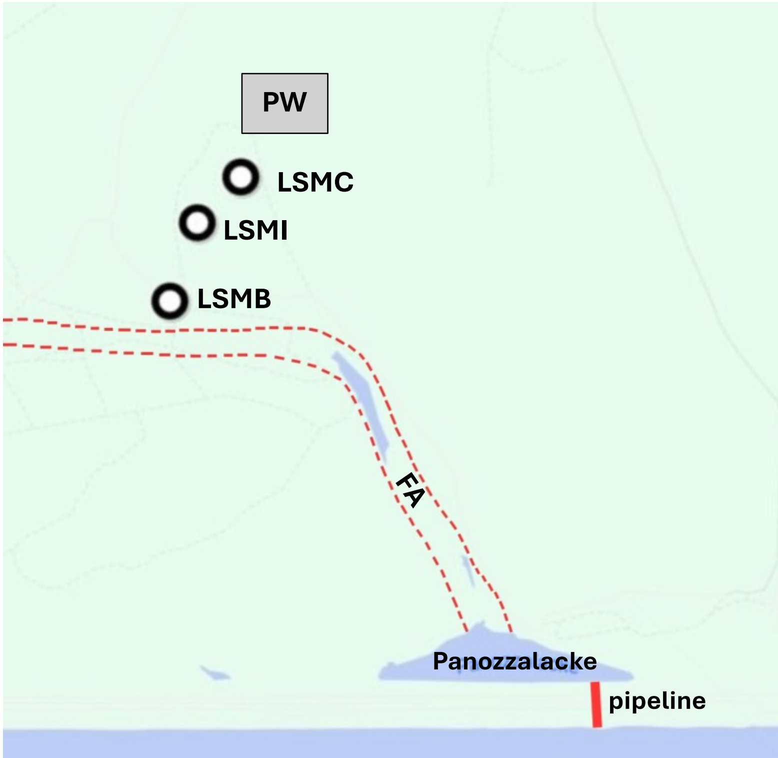

Figure 1. Locations of the monitoring groundwater wells LSMB, LSMI and LSMC, production well Markethäufel (PW), Panozzalacke and Fasangartenarm (FA) (base map: Google Maps; modified by the author). The area between the red dashed lines indicates the zone where surface water is present during donation periods. The pipeline (in red) marks the route through which water flows from the New Danube into the Panozzalacke.

sampling site	coordinates	Well depth (m)
LSMB	48.19048753326454; .48700321829129	7.25 m
LSMI	48.19116946932293;16.4890685778089	14.20 m
LSMC	48.19123143098029;16.4908112336324	13.55 m
Panozzalacke	48.1810830; 16.4876890	
Fasangartenarm	48.190136; 16.486503	

Table 1. Coordinates of sampling sites and well depths for groundwater wells.

2.2. Sampling

The groundwater samples were collected between 06 April 2023 and 23 January 2025 at approximately monthly intervals. Sampling between October 2024 and January 2025 was carried out by the author, while sampling prior to this period was performed by other students and technical assistants. During each sampling, the wells were sampled in a consistent order, starting with LSMC, followed by LSMI and finally LSMB. In addition, surface water samples were taken from the Panozzalacke. At the oxbow channel Fasangartenarm samples were taken when water was present during donation phases.

After opening the well, the dataloggers, which continuously record data for oxygen concentration (DO, mg/L), electrical conductivity (EC, µS/cm), groundwater level (m b.w.h.) and temperature (°C), were removed. At first the groundwater level was measured using an electrical level meter (OTT). Then the fauna sampling was conducted by collecting the stygofauna with a fauna net (mesh size 74 – 100 µm) attached on a string and a fishing rod. A 50 mL Greiner tube and weight were attached to the fauna net to collect the fauna. When the net touched the well bottom, it was lifted up and down ten times for about 1 m before being reeled back . Afterwards, the net was rinsed with tap water to ensure that all captured fauna was transferred into the tube (Jäger & Hahn, 2022). Back in the lab, fauna samples were fixed with Ethanol (70% f. conc.).

Pumping of groundwater was performed using a submersible pump at a flow rate of 3–5 L/min. Pumping was started at 0.5 m below the groundwater level. Before collecting water samples, DO concentration (mg/L), EC (µS/cm), pH and water temperature (°C) were measured by using a MultiLine® Multi 3630 IDS (WTW) multiparameter probe. Once the measured parameters had stabilized, groundwater samples were collected directly from the flowing water during pumping.

For hydrochemistry, analyses three 50 mL Greiner tubes were filled, one unfiltered and the other two filtered through a 0.45 µm filter. One of the two tubes contained 0.2 mL sulfuric acid (H_2SO_4) for later phosphate (PO_4^{3-}) analysis. For hydrogensulfide (HS^-) analysis 5 mL of water were filtered through a 0.45 µm filter into a Greiner tube containing 1 mL of zinc acetate. Additionally, for iron (Fe^{2+}) and manganese (Mn^{2+}) analyses, 5 mL water samples were filtered through a 0.45 µm filter into 15 mL Greiner tubes, each already containing 0.5 mL HCl. For water stable isotope analyses, 15 mL Greiner tubes were filled with untreated water. Similarly, adenosine triphosphatee (ATP) was measured from untreated samples, which were collected in

15 mL Greiner tubes, rinsed prior to sampling. Samples for total cell counts (TCC) were collected in 10 mL Greiner tubes, each already containing glutaraldehyde (0.5 % f. conc.), to ensure immediate fixation. Dissolved inorganic carbon (DIC) samples were collected in combusted 40 mL glass tubes after filtration through a 0.45 µm filter. Samples for dissolved organic carbon (DOC) were collected in a similar way in 40 mL glass tubes, but containing 0.5 mL 1 M HCl. For dissolved organic matter (DOM), samples were collected through a glass fiber filter into a 40 mL pre-combusted glass tube. Additionally, for greenhouse gas analyses, three serum bottles were filled bubble-free. For wastewater indicator analyses, one 100 mL plastic bottle were filled per site. Finally, for microbial community analyses, a 10 L canister was filled with groundwater. During the entire processs of pumping, the water withdrawn from the well was guided through a net with a mesh size of 63 µm to collect fauna that had passed through the submersible pump. Except for the fauna net sampling, these steps were carried out at each groundwater sampling site at two depths, 0.5 m below the groundwater level and 0.5 m above the bottom of the well. The samples were stored dark and cool or refrigerated and frozen until further analyses.

2.3. Analysis

The following analyses were performed on groundwater samples collected during the sampling period. Adenosine triphosphate (ATP) and total cell counts (TCC) measurements were carried out by the author for samples collected between October 2024 and January 2025. The measurements of all the other parameters, as well as ATP and TCC measurements from earlier sampling periods were performed by other students and technical assistants.

2.3.1. Determination of Adenosine Triphosphate (ATP)

The ATP concentration was determined within 1 – 3 days after sampling by means of the BacTiter-Glo™ Assay. First 2 mL water samples from each sampling site were transferred to reaction tubes. Then they were centrifuged for 30 minutes at 4°C at maximum speed. An ATP standard curve was prepared using the following concentrations: 10 nM, 1 nM, 100 pM, 10 pM, 1 pM, and Milli-Q water (MQ) as blank. All standards and samples (180 µL each) were transferred into a 96-well plate prior to the assay measurement. The ATP standard curve was prepared in duplicates, while ATP total and ATP extern concentrations of each sample were measured in triplicates. The BacTiter-Glo™ reagent was thawed and 20 µL were added to each well containing 180 µL of sample or standard. After addition of the BacTiter-Glo™ reagent, the plate was mixed for 20 seconds at 600 rpm and 25 °C using a thermomixer. The luminescence of each well was measured using a GloMax® Navigator (Promega) with an integration time of 0.3 seconds per well. Luminescence data were recorded as relative light units (RLU) and converted to ATP concentrations using the ATP standard curve. Intracellular ATP concentrations were calculated by subtracting extracellular ATP from total ATP. Intracellular ATP can be defined as the available energy within metabolically active cells at a given time. Its production is directly linked to cell growth and metabolic activity, meaning that higher intracellular ATP levels reflect higher biomass and cell volume. When cells become weak or undergo lysis, ATP is released into the surrounding environment. This ATP outside the living cells is reffered to as extracellular ATP (Berthold et al., 2000; Goodsell, 1996; Whalen et al., 2018).

2.3.2. Determination of Total Cell Counts (TCC)

TCC samples were collected directly into tubes pre-amended with glutaraldehyde, resulting in immediate fixation, final concentration of 0.5 %, at the time of sampling. The staining solution (TESG1) was prepared by mixing 999 µL of 10 × TE buffer, filtered through a 0.22 µm filter, with 1 µL of SYBR™ Green I Nucleic Acid Gel Stain (SGI). After preparation the staining solution was stored in the dark until use. For staining, 150 µL of each sample were transferred into a 1.5 mL reaction tube, followed by the addition of 15 µL TESG1. Each sample was prepared in duplicate. After brief mixing, the tubes were incubated for 13 minutes at 37 °C in the dark using a thermomixer. The staining solution binds to both DNA and RNA. Surface water samples were diluted by mixing 135 µL of Milli-Q water with 15 µL of sample, followed by the addition of 15 µL TESG1. Total cell counts were measured using an Amnis® CellStream® (Luminex) Imaging Flow Cytometer (Rieseberg, et al. 2001, Veal et al., 2000).

2.3.3. Greenhouse gas measurement: Carbon Dioxide and Methane

Greenhouse gas measurements were performed using a Cavity Ringdown Spectrometer G2201-i (Picarro), which is equipped with a vacuum pump and a cylinder of synthetic air. The synthetic air, composed of 79.5% nitrogen and 20.5% oxygen, minimizes disturbance of contaminants such as particles and trace gases. For each measurement, two syringes were used, one containing 60 mL of water sample without air and the other containing 120 mL of synthetic air. Subsequently, 60 mL of synthetic air from the other syringe was added to the syringe with the water sample. The water-gas mixture was shaken for one minute and the gas phase was then transferred into the gas syringe, resulting in a final mixture of 60 mL sample gas and 60 mL synthetic air. This mixture was connected to the spectrometer for analysis. Measurements were processed and evaluated using the RShiny app. The headspace volume was 60 mL and the total injected gas volume was 120 mL. Each sample was measured in triplicate to calculate the mean and standard deviation (Habellöcker, 2023).

2.3.4. Measurement of Dissolved organic carbon (DOC) and dissolved inorganic carbon (DIC)

DOC and DIC were measured by using the TOC-L (Shimadzu) TOC analyzer. For the measurement the pre-treatment of the samples and the settings on the device is essential. For the determination of DOC, non-purgeable organic carbon (NPOC) is measured. For this, bottles with a volume of 40 mL were filled using a syringe and a 0.45 µm filter. Prior to analysis, the samples were treated with a 1 M HCl solution. The addition of acid serves a dual purpose: it preserves the samples by inhibiting biological activity and simultaneously reacts with inorganic carbon and converts it to carbon dioxide (Hupach & Bayerl, 2018; Potter & Wimsatt, 2012). Laboratory analysis was carried out shortly after sampling, as delays may lead to different results due to bacterial degradation or oxidation of certain components in the water samples. Additionally, samples were stored at around 4°C and protected from sunlight and exposure to atmospheric oxygen (Mackereth et al., 1989). For the analysis a MQ standard and a calibration curve are required for every measurement. These standards are prepared in 40 mL glass bottles. To prepare the DOC standard 0.25 mL of the DOC standard solution is added to 50 mL of MQ. The DIC standard is prepared by adding 5 mL of the DIC stock solution to 50 mL of MQ. Before each measurement, the instrument's flushing tank was rinsed with MQ and refilled with fresh MQ to prevent contamination. Each water sample is analyzed in duplicate. Following the measurements, additional MQ blanks, reference water samples and another MQ blank that has not been acidified are run. The non-acidified MQ blank serves as a control to verify that the hydrochloric acid used for sample acidification is free from contamination. Finally, the carbon concentration in the water samples is determined by subtracting the carbon content of the blank sample from that of the corresponding water sample (Habellöcker, 2023).

2.3.5. Water chemistry

The concentrations of the anions chloride (Cl^-), sulfate (SO_4^{2-}) and nitrate (NO_3^-) were determined by ion chromatography according to DIN EN ISO 10304-1 (DIN Deutsches Institut für Normung, 2009). The cations sodium (Na^+), potassium (K^+), calcium (Ca^{2+}) and magnesium

(Mg^{2+}) were also analyzed using ion chromatography following OENORM DIN EN ISO 14911 (DIN Deutsches Institut für Normung, 1999). Nitrite (NO_2^-) concentrations were measured photometrically using the diazotization method according to DIN EN 26777 (DIN Deutsches Institut für Normung, 1993). Ammonium (NH_4^+) concentrations were determined photometrically using the indophenol blue method according to DIN 38406-5 (DIN Deutsches Institut für Normung, 1983) and OENORM ISO 7150-1 (Austrian Standards International, 1987). Phosphate (PO_4^{3-}), dissolved phosphorus (P) and total phosphorus (P) were analyzed photometrically following OENORM EN ISO 6878 (Austrian Standards International, 2004). Silicate (SiO_4^{4-}) was measured photometrically according to DIN 38405-21 (DIN Deutsches Institut für Normung, 1990). Iron (Fe^{2+}) and manganese (Mn^{2+}) were also determined photometrically following DIN 38406-1 (DIN Deutsches Institut für Normung, 1983) and DIN 38406-2 (DIN Deutsches Institut für Normung, 1983). Hydrogensulfide (HS^-) was determined photometrically according to DIN 38405-27 (DIN Deutsches Institut für Normung, 2017).

2.3.6. Fauna examination

Fauna samples were examined to determine the groundwater fauna present. Each sample was first poured through a 100 µm filter and rinsed with tap water to remove the ethanol-eosin solution. The filtered material was transferred to a small glass container and subsamples were placed on a petri dish for observation under a binocular. All detected fauna was preserved in Eppendorf tubes containing 96% undenatured ethanol and organized by sampling site, date and taxonomic group. After sorting all individuals, the remaining sediment was returned to a 50 mL Greiner tube, filled with 96% denatured ethanol and stored in a refrigerator. Taxonomic identification was carried out using the identification key *Bestimmung von Evertebraten des Grundwassers* (Gaviria-Melo & Fuchs, 2020).

2.3.7. Statistical data analysis

The data was first divided into two groups based on the sampling date (Table 2), „donation", which contained all samples collected during donation periods, and „no donation", which contained all samples collected during periods without surface water supply.

donation	no donation
29 June 2023	6 April 2023
20 July 2023	20 April 2023
3 August 2023	4 May 2023
21 September 2023	1 June 2023
7 May 2024	16 November 2023
29 May 2024	19 December 2023
18 June 2024	26 January 2024
7 July 2024	29 February 2024
24 October 2024	28 March 2024
	25 April 2024
	5 December 2024
	23 January 2025

Table 2. Sampling dates during donation and no donation periods.

Parts of the data analysis are based on a pipeline developed within the working group by Angela Cukusic and Clemens Karwautz. All data was analyzed in R, version 4.4.2 (R Core Team, 2024). The data structure was displayed using „kable()" from the package „knitr" (Xie, 2024). Data selection and preprocessing were performed using functions from the package „tidyverse" (Wickham et al., 2019), including filtering the sampling sites, differentiating between samples during donation and without donation. All data was tested for normal distribution, by performing the *Shapiro-Wilk-Test* (Shapiro & Wilk, 1965). For the normally distributed data, *Levene test* (Levene, 1960) from the package „car" (Fox & Weisberg, 2019) was subsequently performed to assess the homogeneity of variances. To test for differences between donation periods and periods without donation, a *t*-test (Gosset, 1908) was performed for data that were normally distributed and exhibited homogeneity of variances , while the Wilcoxon test (Wilcoxon, 1945) was applied to non-normally distributed data. The same procedure was used to test for differences between positions within the wells (up and down). To determine differences between the sampling sites LSMB, LSMI, and LSMC, a Kruskal–Wallis test (Kruskal & Wallis, 1952) was performed. Subsequently, a Dunn test (Dunn, 1964) with Holm correction from the package „FSA“ (Ogle et al., 2025) was used to identify which sampling sites differed significantly from each other. The packages „ggplot2“ (Wickham, 2016) and the package „patchwork“ (Pedersen, 2024) were used for visualizing the data. Correlation analyses between selected parameters were performed using Spearman’s rank correlation (Spearman, 1904). The resulting correlation matrices were visualized using the package „corrplot“ (Wei & Simko, 2024). For the Fauna analysis taxonomy, abundance and environmental data were combined into a single object using the package „phyloseq“ (McMurdie & Holmes, 2013). The relative abundance of taxa was visualized using the package „microViz“ (Barnett et al., 2021). The conversion of phyloseq objects to microeco-compatible format was performed using the „file2meco“ package (Liu et al., 2022).

3 Results

3.1. Environmental parameters

3.1.1. Groundwater table

Groundwater levels are reported in meters above Adriatic Sea level (m a.s.l.). Significant differences in water levels were observed among the three monitoring wells ($\chi^2 = 99.6$, df = 2, $p < 0.001$), with post-hoc Dunn tests indicating significant differences between LSMB and LSMI ($p < 0.001$), LSMB and LSMC ($p < 0.001$) and LSMI and LSMC ($p < 0.001$). As shown in Figure 2, LSMC exhibited the lowest average groundwater levels (152.7 ± 0.31 m a.s.l.) and the largest fluctuations among the three sampling sites, ranging from 152.3 to 153.7 m a.s.l. Groundwater tables were 154 ± 0.24 m a.s.l. at LSMB and 153.2 ± 0.24 m a.s.l. at LSMI.

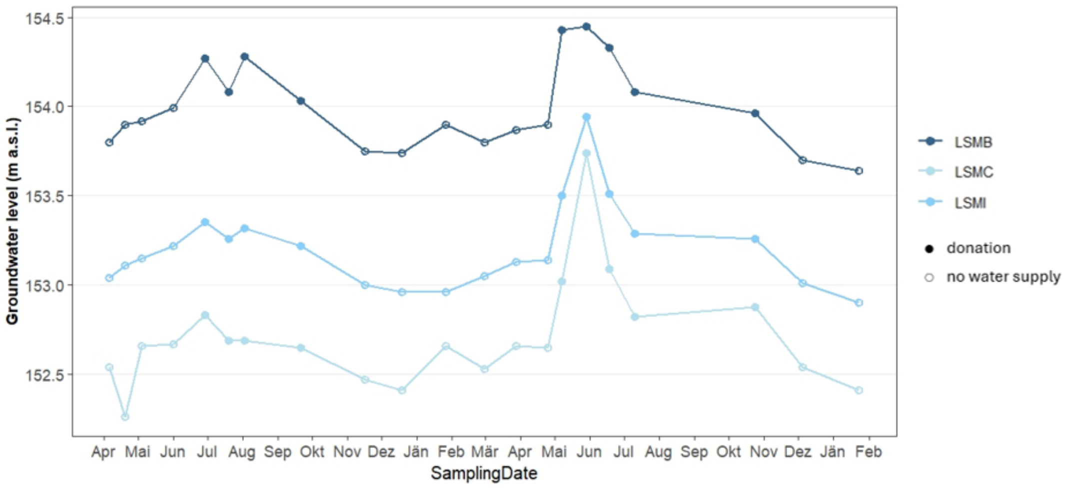

Figure 2 Groundwater levels at LSMB, LSMI, and LSMC (meters above sea level, m a.s.l.). Filled points indicate donation periods.

Groundwater levels differed significantly between donation and non-donation periods in all three wells (LSMB: W = 428, $p < 0.001$; LSMI: W = 430, $p < 0.001$; LSMC: W = 414, $p < 0.001$), showing higher groundwater levels during donation in all three monitoring wells (Figure 3). LSMB and LSMC both increased by 0.4 m due to the donation and LSMI increased by 0.3 m on average. All three wells showed lower groundwater levels during the winter months. Precipitation was summed over the 14 days preceding each sampling date, using daily 24 h cumulative rainfall data from weather station Groß-Enzersdorf (GeoSphere Austria, 2025). Spearman's rank correlation revealed a weak, but non-significant positive relationship between groundwater levels and cumulative precipitation over the preceding 14 days ($\rho = 0.111$, $p = 0.225$).

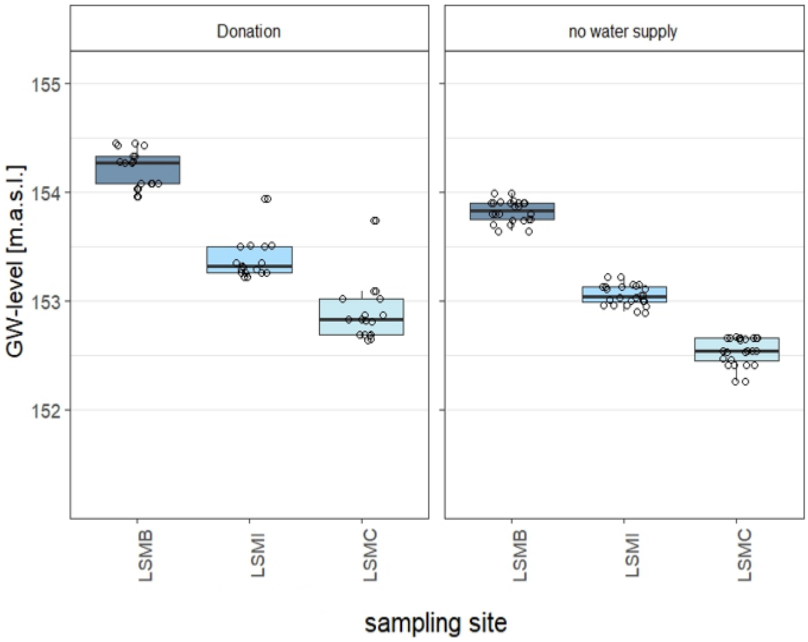

Figure 3. Groundwater levels (m a.s.l.) in the wells LSMB, LSMI, and LSMC during donation (left) and no-donation (right) periods.

3.1.2. Electrical conductivity (EC)

Kruskal-Wallis test revealed no significant differences between LSMB, LSMI and LSMC ($\chi^2 = 1.9$, $df = 2$, $p = 0.386$). For LSMB, the comparison between periods with and without surface water donation revealed a significant difference ($W = 131.5$, $p = 0.033$), with lower values during donation (547.8 ± 46.24 µS/cm) compared to no-donation periods (591.8 ± 49.89 µS/cm). This sampling site exhibited the largest variation in EC, with values between 484 and 623 µS/cm. LSMC, in contrast, showed relatively constant EC values throughout the sampling period (565 ± 21.6 µS/cm) with no significant changes during donation ($W = 238.5$, $p = 0.576$), while LSMI showed even lower variability (572 ± 13.9 µS/cm) and also no significant effect of donation ($W = 206.5$, $p = 0.819$). The EC values of the two surface water bodies Panozzalacke and Fasangartenarm were significantly lower ($W = 3220.5$, $p < 0.001$) than the EC values of the groundwater (Figure 5a). Within the Panozzalacke, EC values were significantly lower during surface water donation, compared to periods without donation ($W = 13$, $p = 0.03$), indicating lower EC values in the New Danube.

3.1.3. Dissolved Oxygen (DO)

LSMC differed significantly from the other two groundwater sampling sites, LSMB and LSMI (LSMC – LSMB $p < 0.001$, LSMC – LSMI $p < 0.001$), exhibiting the highest average DO concentrations among all three sampling sites (0.81 ± 0.64 mg/L). LSMB averaged 0.39 ± 0.70 mg/L and LSMI averaged 0.25 ± 0.23 mg/L. Additionally, a significant difference in DO between positions within the well (up vs. down) was observed at LSMC ($W = 100$, $p = 0.003$), with higher concentrations in the upper position, i.e. 0.5 m below the groundwater table. Notable peak values were recorded in November 2023 at LSMB (max 3.45 mg/L) and LSMI (max 1.12 mg/L) at the same time, whereas at LSMC the highest values were recorded in May and June 2024 (Figure 4). No significant differences in DO were observed between donation and periods without surface water supply across all three groundwater sampling sites (LSMB: $W = 198.5$, $p = 0.665$; LSMI: $W = 159$, $p = 0.15$; LSMC: $W = 248.5$, $p = 0.416$). The surface water exhibited significantly higher DO concentrations ($W = 41$, $p < 0.001$) than groundwater with the Panozzalacke ranging from 4 to 15.7 mg/L and the Fasangartenarm from 0.65 to 13.2 mg/L over the entire monitoring period (Figure 5b).

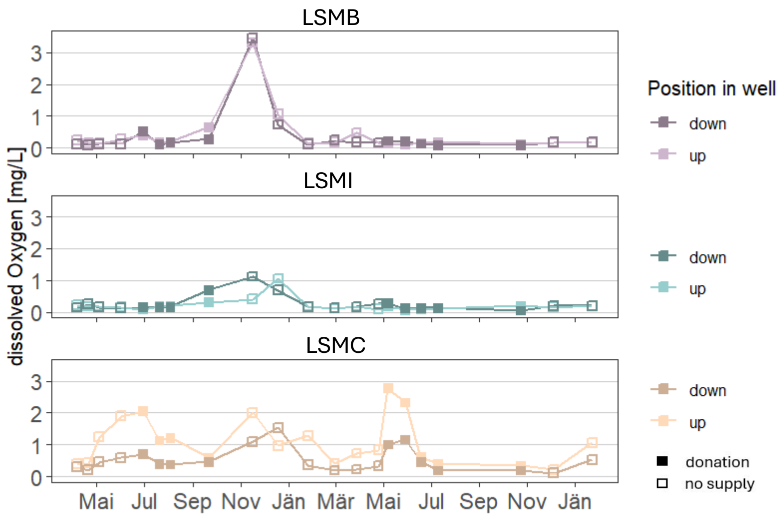

Figure 4. Dissolved oxygen (mg/L) in gw over time at the three monitoring wells showing measurements at both well positions (up and down). Filled squares indicate surface water donation periods.

3.1.4. Temperature

Groundwater temperature across all three monitoring wells ranged from 10.1 °C to 18.8 °C during the monitoring period, with the greatest seasonal difference observed at LSMB (8.72 °C). LSMI differed significantly from the other two groundwater wells (LSMB – LSMI: $p < 0.001$; LSMC – LSMI: $p < 0.001$), while LSMB and LSMC did not differ significantly ($p = 0.494$). Average groundwater temperatures were lowest at LSMI (11.5 ± 0.23 °C), compared to LSMB (13.3 ± 0.07 °C) and LSMC (12.2 ± 0.64 °C). All three wells showed their lowest temperatures at the end of April/early May, with lower values in spring 2023 compared to spring 2024 and the highest temperatures during summer and autumn (LSMB max 18.8 °C on 21 September 2023, LSMC max 13.7 °C on 24 October 2024). The surface water Panozzalacke showed seasonal temperature fluctuations, ranging from 1.5 °C to 26.9 °C with the highest temperature recorded on 20 July 2023 and the lowest on 23 January 2025. Significant differences between donation and non-donation phases were detected at LSMB ($W = 301$, $p = 0.033$) and LSMI ($W = 320$, $p = 0.009$), with higher temperatures during donation (LSMB: 14.2 ± 2.46 °C; LSMI: 11.6 ± 0.24 °C) , whereas no significant effect of donation was observed at LSMC ($W = 292$, $p = 0.056$; Figure 5c).

3.1.5. pH

The pH values remained relatively stable throughout the entire investigation period, with one notable peak at LSMB on 18 June 2024, reaching a maximum of 10.7. Across the groundwater wells, pH values were in the neutral to slightly basic range (LSMB 7.64 ± 0.61; LSMI 7.52 ± 0.24; LSMC 7.41 ± 0.15). LSMC differed significantly from both LSMB ($p = 0.008$) and LSMI ($p < 0.001$) , while no significant difference was found between LSMB and LSMI ($p = 0.795$). Similarly, the Fasangartenarm displayed average pH values of 7.58 ± 0.39 and did not differ significantly from any of the groundwater wells (Fasan–LSMB: $p = 0.598$; Fasan–LSMI: $p = 0.909$; Fasan–LSMC: $p = 1$). In contrast, the surface water of the Panozzalacke exhibited higher pH values (8.12 ± 0.28) compared to groundwater and differed significantly from all groundwater sampling sites ($p < 0.001$). Within the groundwater wells, no significant differences were observed between donation and non-donation periods in LSMB ($W = 180$, $p = 0.366$), LSMI ($W = 227$, $p = 0.789$) and LSMC ($W = 177$, $p = 0.325$; Figure 5d).

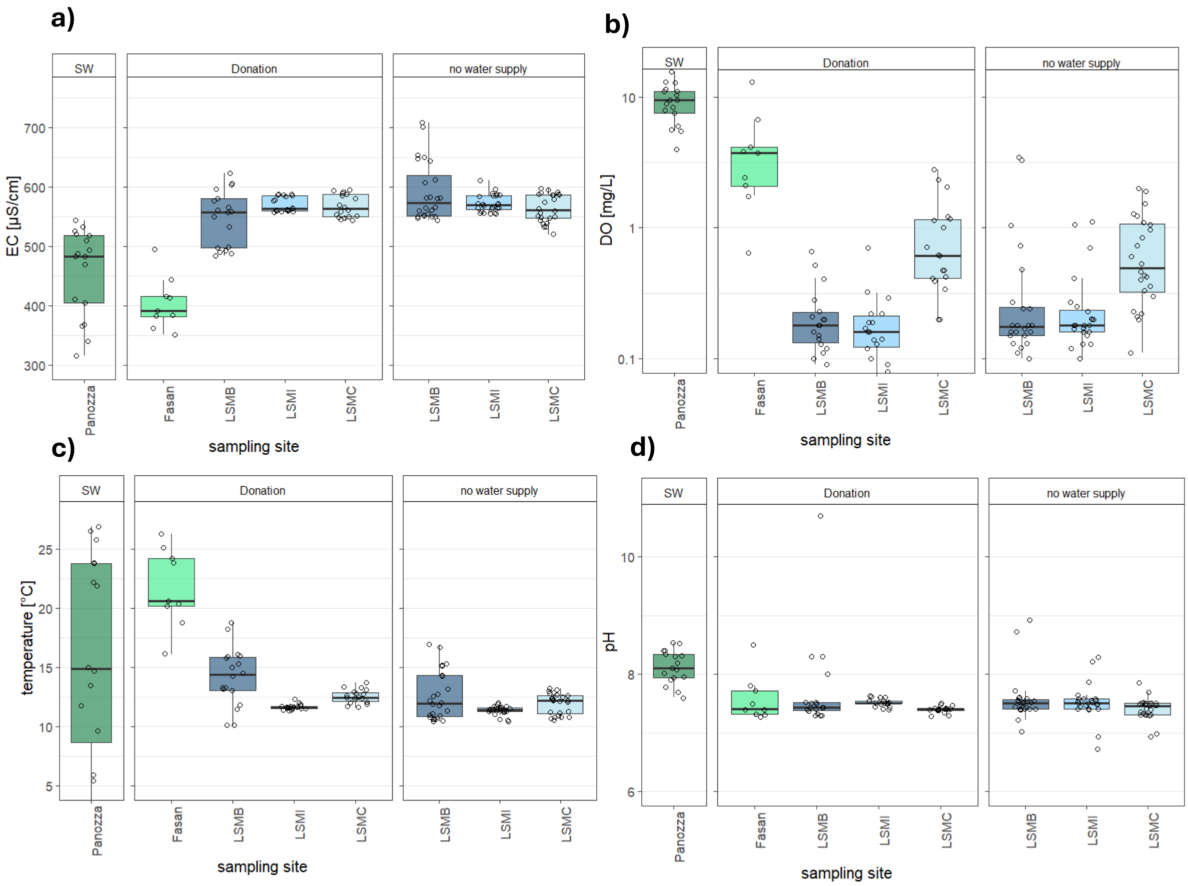

Figure 5. Boxplots of a) electrical conductivity (EC), b) dissolved oxygen (DO, logarithmic scale), c) temperature, and d) pH. The box of Panozzalacke is based on all samples collected across the entire monitoring period. In the ‚Donation' plot the surface water Fasangartenarm (Fasan) is included, which only contained surface water during donation periods.

3.2. Major ions

Among the three groundwater wells LSMI consistently exhibited the highest concentrations and lowest variability for magnesium (Mg^{2+}; 18.7 ± 0.87 mg/L) and sodium (Na^{+}; 17.8 ± 4.36 mg/L). For both ions, LSMI differed significantly from the other two wells. Mg^{2+} concentrations in LSMI were significantly higher than in LSMB ($p < 0.001$) with an average of (17.6 ± 2.2 mg/L) and in LSMC ($p < 0.001$) with an average of (17.7 ± 1.15 mg/L). The difference in Na^{+} concentrations between LSMI and the other two wells was also significant (LSMI – LSMB: $p = 0.004$; LSMI – LSMC: $p = 0.005$). A similar pattern was observed for chloride (Cl^{-}). LSMI showed significantly higher Cl^{-} concentrations than LSMC ($p = 0.013$), with average values of 20 ± 2.2 mg/L in LSMI compared to LSMC (18.2 ± 2.7 mg/L). Chloride concentrations did not differ significantly in LSMB and LSMC ($p = 0.305$) nor between LSMB and LSMI ($p = 0.137$). The two groundwater wells LSMB and LSMC generally showed lower concentrations and higher variability across these ions, indicating that LSMI provides the most stable conditions of the three sampling sites. Calcium (Ca^{2+}) concentrations also varied among the groundwater wells. LSMC differed significantly from LSMI ($p = 0.001$), while LSMB did not differ significantly from LSMI ($p = 0.064$) or LSMC ($p = 0.163$). LSMC exhibited the highest Ca^{2+} concentrations of all three groundwater wells (73.1 ± 4.23 mg/L), while LSMI showed the lowest and most stable values (69.5 ± 3.71 mg/L). LSMB exhibited the highest variability (72.1 ± 6.6 mg/L) in Ca^{2+} concentrations. Also SiO_4^{4-} concentrations differed significantly among the three groundwater wells (LSMB–LSMI: $p < 0.001$; LSMB–LSMC: $p = 0.01$; LSMI–LSMC: $p < 0.001$). LSMI exhibited the lowest and most stable SiO^{4-} concentrations (9.75 ± 0.15 mg/L), whereas LSMC showed the highest values (10.9 ± 0.38 mg/L). LSMB showed intermediate concentrations (10.8 ± 1.18 mg/L) but the highest variability. No significant differences in potassium (K^{+}) concentrations were observed among the sampling sites, including both groundwater and surface water ($\chi^2 = 6.24$, df = 4, $p = 0.182$), with values ranging from 2.2 to 4.1 mg/L.

Calcium and magnesium concentrations in the two surface water sites Panozzalacke and Fasangartenarm did not differ significantly from each other (Ca^{2+}: $p = 0.484$; Mg^{2+}: $p = 0.775$). Both ions showed significantly lower concentrations in surface water compared to the groundwater wells (Ca^{2+}: W = 3432.5, $p < 0.001$; Mg^{2+}: W = 3278.5, $p < 0.001$). The average surface water concentration of Ca^{2+} during the sampling period was (50.5 ± 11.1 mg/L) and Mg^{2+} (14.4 ± 1.7 mg/L; Figure 6). Silicate concentrations in the surface waters differed significantly from each other, with higher values in the Panozzalacke (11.6 ± 6.37 mg/L) than in the Fasangartenarm (7.46 ± 4.24 mg/L; $p = 0.003$). Fasangartenarm differed significantly from LSMB ($p = 0.002$) and LSMC ($p < 0.001$), while Panozzalacke only differed significantly from LSMI ($p = 0.008$).

Surface water donation had a measurable effect on magnesium concentrations at LSMB, where values were significantly lower during periods of surface water input (16.2 ± 1.54 mg/L) compared to periods without donation (18.6 ± 2.05 mg/L; $t = -4.24$, $df = 40$, $p < 0.001$; Figure 6b). In contrast, the other groundwater wells LSMC and LSMI remained unaffected (LSMI: $W = 199$, $p = 0.67$; LSMC: $W = 228$, $p = 0.77$). No significant effects of surface water donation were observed for Ca^{2+}, Na^+, K^+ and Cl^- at any of the three groundwater wells (see Table 3 in Appendix). During the sampling period, Na^+ and K^+ concentrations declined in all three groundwater wells (Figure 7) and in the Panozzalacke, particularly from July 2024 onwards.

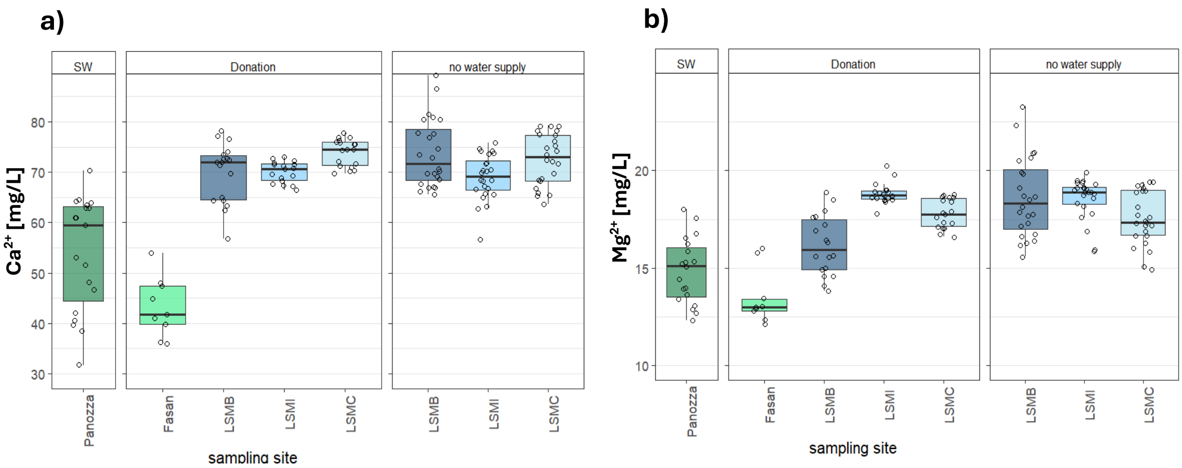

Figure 6. Boxplots of a) calcium (Ca^{2+}), b) magnesium (Mg^{2+}). The box of Panozzalacke (Panozza) is based on all samples collected across the entire monitoring period. In the ‚Donation' plot the surface water Fasangartenarm (Fasan) is included, which only contained surface water during donation periods.

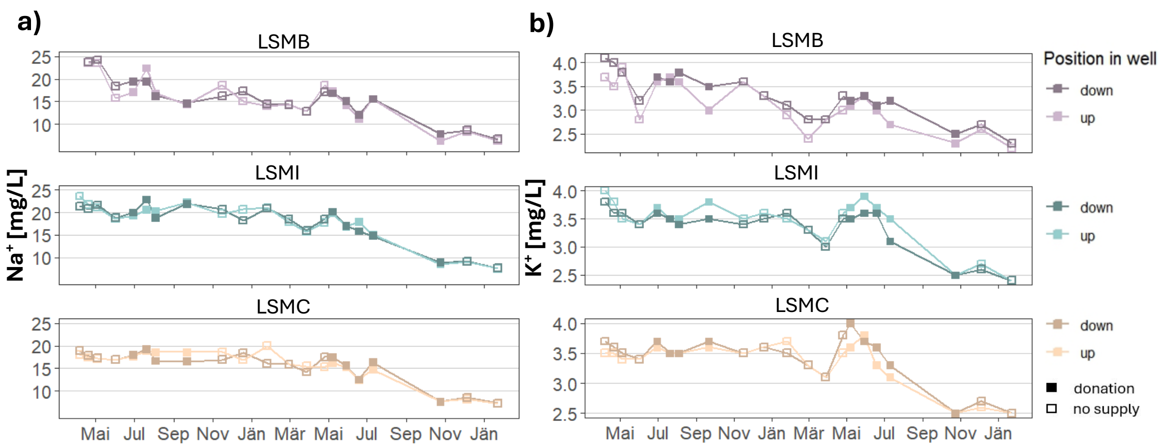

Figure 7 a) Sodium (Na^+) and b) potassium (K^+) over time at the three groundwater wells showing measurements at both well positions (up and down). Filled squares indicate surface water donation.

3.3. Nutrients

3.3.1. Ammonium (NH_4^+)

No significant differences between donation and non-donation periods were found at LSMB (W = 178.5, p = 0.347) or LSMI (t = -1.6, df = 40, p = 0.117). In contrast, LSMC showed a significant difference between donation and periods without water supply (t = -2.69, df = 40, p = 0.01), with lower concentrations during donation (21.8 ± 12.2 µg/L) compared to non-donation periods (33.7 ± 15.5 µg/L). All groundwater wells differed significantly from each other (LSMB–LSMC p = 0.047; LSMB–LSMI p < 0.001; LSMC–LSMI p < 0.001). LSMI exhibited the highest and most stable concentrations (45.4 ± 10.8 µg/L), whereas LSMB had the lowest mean value but the highest variability (37.7 ± 97.3 µg/L). The maximum values at all three groundwater wells were detected on the first sampling date 4 April 2023 (LSMB: 632 µg/L; LSMI: 74 µg/L; LSMC: 57 µg/L). At all three sampling sites concentrations declined during summer 2023, followed by a slight increase afterwards. Ammonium concentrations declined again in LSMI and LSMC during the summer months in 2024, a similar trend was visible in Panozzalacke. A significant difference between the upper and lower sampling position was observed at LSMC (W = 341.5, p = 0.002), with higher concentrations at the lower position (36.1 ± 11.3 µg/L) than at the upper position (21.1 ± 15.1 µg/L) and a noticeable decline at the upper position during the summer months (Figure 8a).

A significant difference was also observed between groundwater and surface water (W = 1223.5, p = 0.011). Panozzalacke had an average NH_4^+ concentration of 79.9 ± 77.5 µg/L, while Fasangartenarm had an average of 41.6 ± 27 µg/L. Both surface waters did not differ significantly from each other (W = 63.5, p = 0.415). Panozzalacke showed seasonal fluctuations with higher values in winter than in summer.

3.3.2. Phosphate (PO_4^{3-})

Orthosphate concentrations did not differ significantly between donation periods and periods without surface water supply at any of the groundwater wells (LSMI W = 236, p = 0.308; LSMB W = 152.5, p = 0.221; LSMC W = 187, p = 0.775). All three wells differed significantly from each other (p < 0.001), with LSMI exhibiting the highest concentrations (61 ± 12.8 µg/L), LSMC the lowest (18.5 ± 10.4 µg/L) and LSMB intermediate (43.3 ± 17.9 µg/L). All three wells showed an increase in October 2024, with LSMB reaching the maximum of 91.8 µg/L and LSMC 52.9 µg/L. The highest value in LSMI was measured on 20 April 2024 (104 µg/L).

A difference for the concentration of PO_4^{3-} in LSMC between position up and down inside the well was observed ($W = 353.5$, $p < 0.001$), with higher concentrations in the lower sampling position (23.6 ± 9.33 µg/L) than in the upper position (12.3 ± 7.36 µg/L). A seasonal variation in LSMC was also observed, with declining concentrations during the summer months (Figure 8b). In LSMB no PO_4^{3-} was detected on 19 December 2023. Surface water exhibited significantly lower PO_4^{3-} concentrations than the groundwater ($W = 3258.5$, $p < 0.001$), with Panozzalacke averaging 5.07 ± 3.69 µg/L and Fasangartenarm 3.2 ± 1.48 µg/L.

3.3.3. Total Phosphorus (P)

Total phosphorus concentrations also differed significantly between groundwater wells (LSMB - LSMC $p < 0.001$; LSMB - LSMI $p = 0.003$; LSMC -LSMI $p < 0.001$), with LSMI showing the highest mean value (23 ± 3.33 µg/L), LSMB intermediate (19 ± 4.64 µg/L) and LSMC the lowest with extremely high variability (13.2 ± 25.3 µg/L). No significant differences were observed between donation and periods without donation at any well (LSMB $W = 122$, $p = 0.112$; LSMI $W = 232.5$, $p = 0.073$; LSMC $W = 193.5$, $p = 0.613$). At LSMC, a significant vertical difference was detected ($W = 270$, $p = 0.009$), with higher concentrations in the lower position (24.6 ± 9.33 µg/L) than in the upper position (12.3 ± 7.36 µg/L; Figure 8c), similar to the pattern observed for PO_4^{3-}. Surface water concentrations were significantly higher than in groundwater ($W = 177.5$, $p = 0.002$), with Panozzalacke averaging 33.9 ± 11.8 µg/L and Fasangartenarm 22.2 ± 8.22 µg/L. Temporal trends were similar to PO_4^{3-}, with a peak observed in all three wells on 24 October 2024 (LSMB max 33.2 µg/L; LSMI max 33.2 µg/ L; LSMC max 164 µg/L).

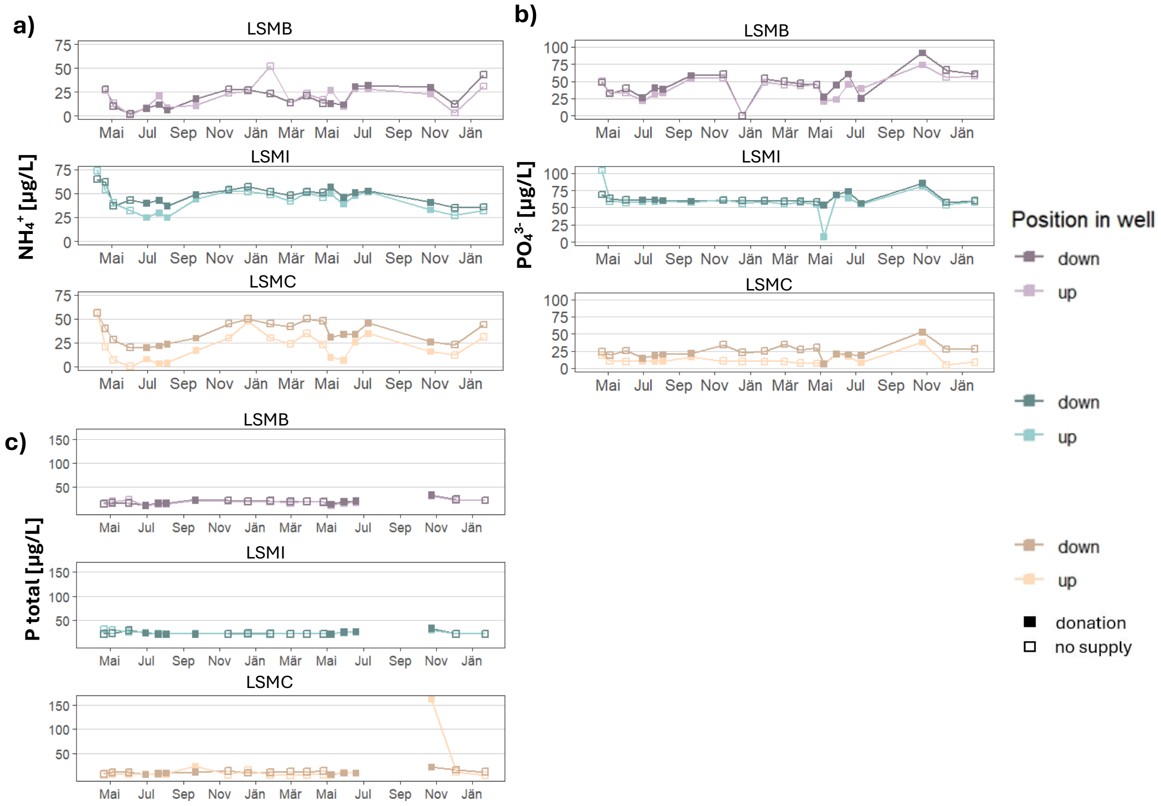

Figure 8 a) Ammonium (NH_4^+), b) Phosphate (PO_4^{3-}) and c) total phosphorus (P total) over time at the three groundwater wells showing measurements at both well positions (up and down). Filled squares indicate surface water donation periods.

3.4. Redox sensitive parameters

3.4.1. Nitrate (NO_3^-)

Nitrate concentrations in the groundwater remained below the detection limit for long periods. Between June 2023 and July 2024, all wells consistently showed nitrate concentrations below the detection limit and this pattern persisted in several subsequent samples. Due to the high number of measurements below the detection limit, the three groundwater monitoring wells did not differ significantly from each other ($\chi^2 = 3.93$, df = 2, p = 0.14). No significant difference between donation periods and periods without water supply was detected in all three sampling sites (LSMB W = 182.5, p = 0.168; LSMI W = 207, p = 0.413, LSMC W = 189, p = 0.132). No significant difference was observed between surface water and groundwater (W = 1642, p = 0.254). In the surface water of the Panozzalacke NO_3^- concentrations ranged from nitrate below the detection limit to 1.6 mg/L, while the Fasangartenarm consistently showed concentrations below to detection and groundwater values ranged from below to detection to 2.20 mg/L. All three groundwater wells, as well as Panozzalacke showed a peak on 4 May 2023 (Figure 9a). This was the only time NO_3^- was detected in LSMI (1.1 mg/L), while LSMB and LSMC reached their maximum on the same date (2.2 mg/L and 1.2 mg/L, respectively).

3.4.2. Nitrite (NO_2^-)

Comparisons between wells revealed no significant difference between LSMB and LSMC (p = 0.145), but both differed significantly from LSMI (LSMB–LSMI p < 0.001; LSMC–LSMI p = 0.023). Average NO_2^- concentrations were highest at LSMI (1.29 ± 2.8 µg/L), followed by LSMB (1.15 ± 0.76 µg/L) and LSMC (1.11 ± 0.6 µg/L). A clear difference was found between surface water and groundwater (W = 294, p < 0.001). Surface waters, particularly the Panozzalacke exhibited higher average NO_2^- concentrations and more variable values (13 ± 16.5 µg/L) than the groundwater wells. Fasangartenarm showed lower mean concentrations (3.73 ± 2.14 µg/L) and did not differ significantly from the Panozzalacke (W = 65, p = 0.461).

Nitrite concentrations at LSMB differed significantly between donation and non-donation periods (W = 295, p = 0.045). Concentrations were higher during donation (1.63 ± 0.91 µg/L) than during periods without surface water supply (0.9 ± 0.57 µg/L). In LSMB a significant difference (W = 122, p = 0.013) regarding the position in the well was also found, with higher concentrations in the upper position (1.3 ± 0.9 µg/L) compared to the lower position (0.9 ± 0.42 µg/L). No significant differences comparing donation without donation periods were found at

LSMI (W = 256, p = 0.304) and LSMC (W = 269, p = 0.177), although both wells slightly increased during donation phases. The highest values across all groundwater wells were recorded on 20 July 2023 during the first donation phase and on 24 October 2024 during the second donation phase. In LSMI the upper position reached a peak (18.7 µg/L) on 3 August 2023. The lower position of LSMC showed an increase during the donation period in 2024 (Figure 9b). Overall, NO_2^- concentrations tended to be lower during winter and spring months.

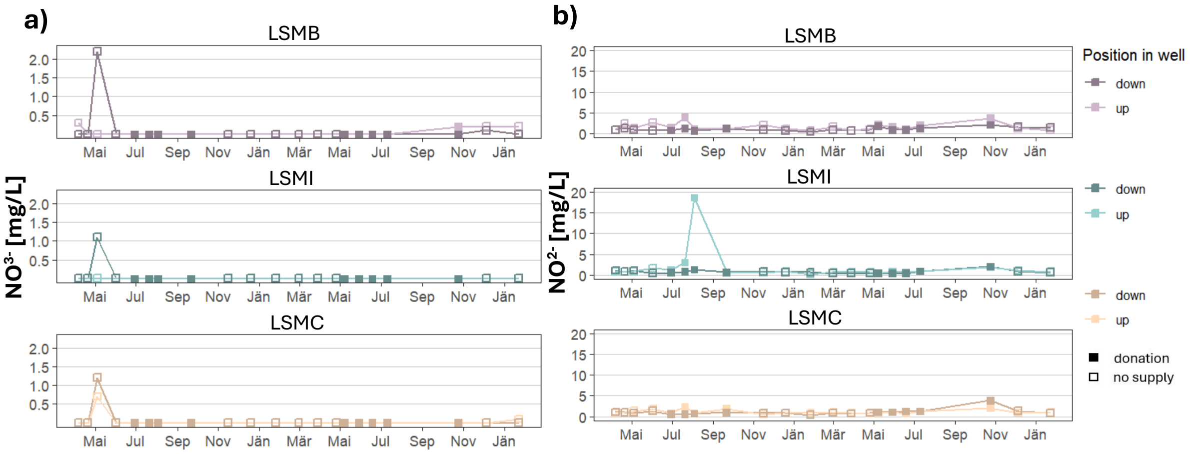

Figure 9. a) Nitrate (NO_3^-) and b) nitrite (NO_2^-) over time at the three groundwater wells showing measurements at both well positions (up and down). Filled squares indicate surface water donation periods.

3.4.3. Sulfate (SO_4^{2-})

LSMI exhibited significantly higher concentrations of SO_4^{2-} than LSMB ($p < 0.001$) and LSMC ($p < 0.001$). LSMI showed the highest average values (12.9 ± 2.24 mg/L), followed by LSMB (10.2 ± 5.89 mg/L) and LSMC had the lowest SO_4^{2-} concentrations (8.86 ± 3.94 mg/L). Surface water donation significantly affected LSMB (W = 94.5, p = 0.002), but not the other two sampling sites (LSMI: W = 250.5 p = 0.387; LSMC: W = 158, p = 0.144; Figure 10). Sulfate concentrations in LSMB were lower during donation periods (7.65 ± 5.64 mg/L) than during periods without surface water supply (12.2 ± 5.4 mg/L). SO_4^{2-} concentrations also differed significantly between donation and non-donation periods in the Panozzalacke (W = 77.5, p = 0.01), with higher values observed during donation (14 ± 5.28 mg/L) compared to periods without donation (6.86 ± 4.49 mg/L).

Panozzalacke and Fasangartenarm did not differ significantly from each other (p = 0.267) showing concentrations between 3.40 and 20.8 mg/L. Only the sulfate concentrations in LSMI differed significantly from the Panozzalacke (p = 0.048), while LSMC differed significantly from the Fasangartenarm (p = 0.023). At LSMI, SO_4^{2-} concentrations showed a continuous decline over the sampling period, starting at 15.5 mg/L at the first sampling and reaching concentrations between 7.8 and 8.7 mg/L on the last two sampling dates. LSMB exhibited the highest sulfate values in spring, followed by a decrease during donation phases. LSMC showed a similar trend, but weaker than in LSMB. Both LSMB and LSMC declined from May 2024 onward and displayed the lowest values toward the end of the monitoring period (Figure 11a).

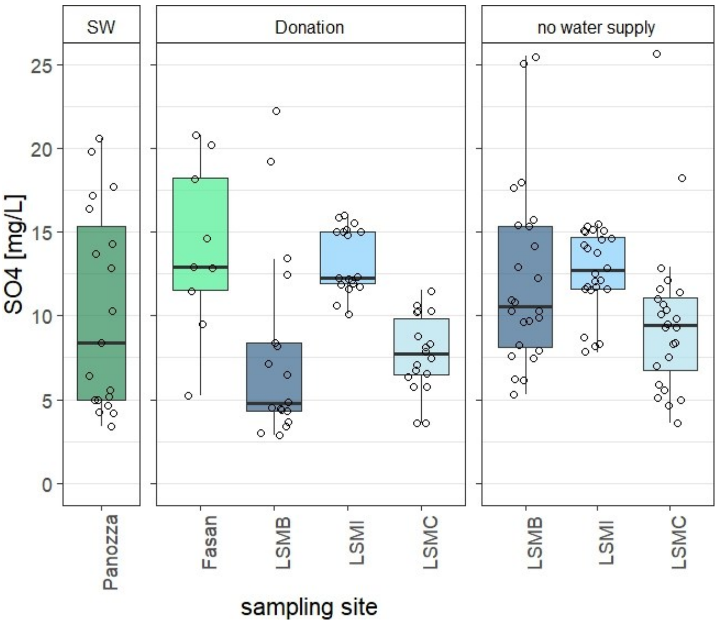

Figure 10 Boxplots of Sulfate (SO_4^{2-}) The box of Panozzalacke (Panozza) is based on all samples collected across the entire monitoring period. In the ‚Donation‘ plot the surface water Fasangartenarm (Fasan) is included, which only contained surface water during donation periods.

3.4.4. Sulfide (HS^-)

Sulfide concentrations did not differ significantly between the three groundwater sampling sites ($\chi^2 = 0.72$, df = 2, p = 0.7). Also no significant difference between donation and periods without surface water supply was observed across the groundwater sampling sites (LSMB: W = 206.5, p = 0.828; LSMI: W = 221, p = 0.54; LSMC: W = 212.5, p = 0.517). Panozzalacke and Fasangarten did not differ from each other (p = 1). The groundwater concentrations differed significantly from the surface water (W = 2928.5, $p < 0.001$). Surface water values ranged from 0 to 0.14 mg/L and groundwater from 0 – 0.9 mg/L. HS^- concentrations showed the opposite pattern of SO_4^{2-} from May 2024 onward, with increasing values and the highest concentrations recorded at the end of the monitoring period (Figure 11a,b).

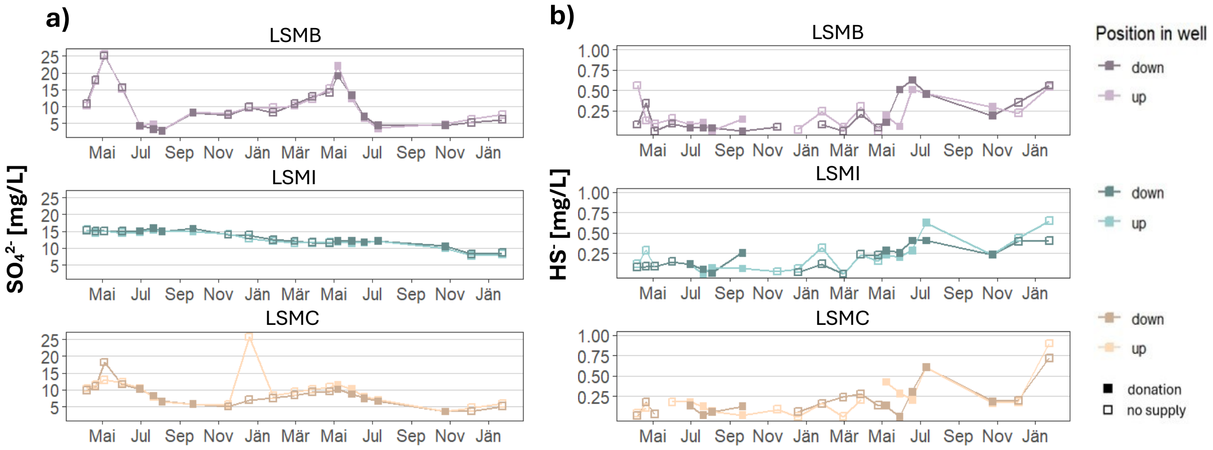

Figure 11 a) Sulfate (SO_4^{2-}) and b) sulfide (HS^-) over time at the three groundwater wells showing measurements at both well positions (up and down). Filled squares indicate surface water donation periods.

3.4.5. Iron (Fe^{2+})

Iron concentrations differed significantly among the three groundwater sampling sites (LSMB – LSMI: $p < 0.001$; LSMB – LSMC: $p = 0.001$; LSMI – LSMC: $p < 0.001$). Over the entire monitoring period, LSMI exhibited the highest Fe^{2+} concentrations (1.61 ± 1.06 mg/L), followed by LSMB (868 ± 587 µg/L) and LSMC (400 ± 565 µg/L). All three wells reached their maximum concentrations on 3 August 2023 (LSMB 3.41 mg/L; LSMI 6.36 mg/L; LSMC 2.77 mg/L). In LSMC, significant differences between the upper and lower well position were detected ($W = 429$, $p = 0.001$). The lower position showed higher concentrations (754 ± 620 µg/L) compared to the upper position (45.8 ± 77.7 µg/L). While concentrations at the upper position remained relatively stable, the lower position exhibited higher fluctuations (Figure 12a).

No significant differences between donation and periods without donation were found in LSMB ($W = 181$, $p = 0.385$) and LSMC ($W = 198$, $p = 0.656$), although an increase in Fe^{2+} concentrations was visible during the donation period in 2023. During donation 2024, LSMB and LSMC showed very low Fe^{2+} concentrations from May to July, followed by a slight increase in the second half of the donation period (Figure 12a). LSMI showed significantly higher concentrations during the donation period ($W = 118$, $p = 0.013$), with mean concentrations of 1.88 ± 1.6 mg/L during donation and 1.41 ± 0.06 mg/L without donation. It is important to note that these elevated concentrations occurred only during donation in 2023. During donation 2024 Fe^{2+} concentrations were low in LSMI.

Surface water data were incomplete for several sampling dates. The available measurements showed significantly lower Fe^{2+} concentrations in surface water compared to the groundwater

(W = 743, p = 0.002). Panozzalacke had mean Fe^{2+} concentrations of 87 ± 40.9 µg/L, and Fasangartenarm 212 ± 5.2 µg/L.

3.4.6. Manganese (Mn^{2+})

Manganese concentrations differed significantly between the groundwater sampling sites. LSMB exhibited lower concentrations compared to both LSMC (p = 0.001) and LSMI (p = 0.009), while no significant difference was observed between LSMC and LSMI (p = 0.517). LSMC shows the highest concentration and variability (408 ± 317 µg/L), followed by LSMI (369 ± 275 µg/L) and LSMB with the lowest concentrations (265 ± 174 µg/L). Similar to iron, in LSMC significant differences between the upper and lower position in the well were observed for manganese (W = 429, p = 0.024), with higher concentrations in the lower position (498 ± 301 µg/L) than in the upper position (319 ± 315 µg/L; Figure 12b). In LSMB, manganese concentrations differed significantly between donation and periods without donation (W = 122, p = 0.017), with elevated values and a peak during the first donation phase, but low values during the donation period in 2024. In LSMC and LSMI no significant differences were found between donation and non-donation periods (LSMC: W = 167.5, p = 0.223; LSMI: W = 177.5, p = 0.334) , although a peak during the first donation phase is visible. Manganese concentrations followed the same dynamics as iron with higher values in the donation period 2023 and low concentrations at the beginning of the donation period 2024 and a slight increase in the second half of donation 2024 (Figure 12b).

Surface water concentrations did not differ significantly from the groundwater (W = 592, p = 0.129). As with iron, many surface water measurements were missing.

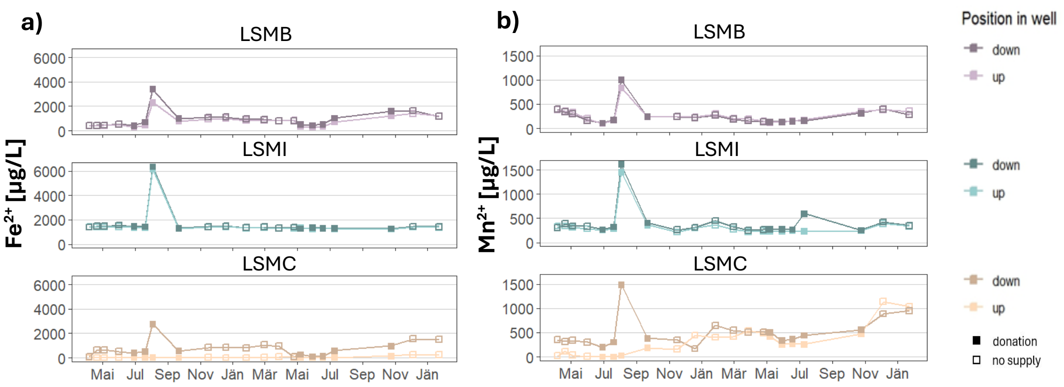

Figure 12 a) Iron (Fe^{2+}; µg/L) and b) manganese (Mn^{2+}; µg/L) over time at the three groundwater wells showing measurements at both well positions (up and down). Filled squares indicate periods of donation.

3.5. Carbon species

3.5.1. Dissolved organic carbon (DOC)

In terms of DOC, all groundwater sampling sites differed significantly from each other (LSMB – LSMI: $p < 0.001$; LSMB – LSMC: $p = 0.02$; LSMC – LSMI: $p = 0.012$). DOC concentrations differed significantly between donation and non-donation periods at LSMB ($W = 378$, $p < 0.001$) and LSMI ($W = 98.5$, $p = 0.008$), whereas no significant difference between donation and non-donation periods was detected at LSMC ($W = 159.5$, p-value = 0.155). At LSMB, DOC concentrations were higher during donation periods (2.11 ± 0.31 mg/L) compared to periods without donation (1.30 ± 0.46 mg/L). In contrast, LSMI showed lower DOC concentrations during donation (0.95 ± 0.17 mg/L) compared to periods without donation (1.2 ± 0.36 mg/L; Figure 13a). The lowest concentrations at LSMB occurred between December 2023 and the end of April 2024, ranging from 0.79 to 1.05 mg/L. The maximum DOC concentration at LSMB was recorded on 21 September 2023, reaching 2.89 mg/L. At LSMC, DOC concentrations averaged 1.29 ± 0.39 mg/L, placing this sampling site between LSMB and LSMI in terms of DOC concentration levels. A peak in the lower position of LSMC occurred on 6 June 2023, with a maximum value of 2.8 mg/L. This increase was only detected at the lower position in the well, while the upper position showed no corresponding increase.

Surface water had significantly higher DOC concentrations compared to groundwater ($W = 11$, $p < 0.001$). Fasangartenarm and Panozzalacke did not differ significantly from each other ($p = 0.79$) and exhibited concentrations ranging between 2.35 and 6.01 mg/L.

3.5.2. Dissolved inorganic carbon (DIC)

DIC concentrations differed only partially among the groundwater sampling sites and diffferences were found minor . However, LSMI showed significantly lower concentrations than LSMC ($p = 0.009$). No significant differences were observed between LSMB and LSMI ($p = 0.068$) and between LSMB and LSMC ($p = 0.40$). LSMC exhibited the highest average concentration of all three wells (62.2 ± 9.81 mg/L), while LSMI showed the lowest (59.6 ± 8.89 mg/L). The concentration of LSMB was between the two wells and showed the highest variability (61.2 ± 12.6 mg/L). All three wells reached their maximum DIC concentration on 29 June 2024 (LSMB: 105 mg/L; LSMI: 93 mg/L; LSMC: 97.1 mg/L). Surface water donation had no significant effect on DIC concentrations at any of the three wells (LSMB: $W = 127$, $p = 0.107$; LSMI: $W = 138$, $p = 0.14$; LSMC: $W = 171$, $p = 0.721$). However, at LSMB there was a decrease in DIC during the donation periods, although this trend was not statistically significant (Figure 13b). Surface water differed significantly from groundwater ($W = 1816.5$, $p < 0.001$). Mean concentrations were 48.6 ± 8.65 mg/L in Panozzalacke and 38.8 ± 11.7 mg/L in Fasangartenarm. The two surface water bodies did not differ significantly from each other ($W = 23$, $p = 0.339$). A significant difference between donation and non-donation periods was observed in the Panozzalacke ($t = -3.86$, $p = 0.005$). DIC concentrations were higher during non-donation periods (54 ± 2.27 mg/L) compared to donation periods (40.5 ± 8.36 mg/L).

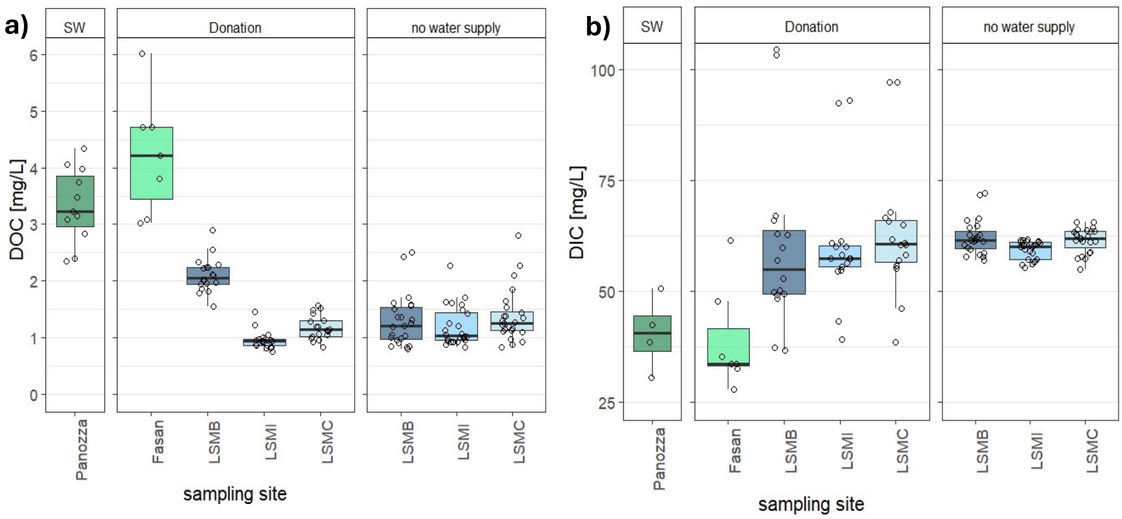

Figure 13. Boxplots of a) dissolved organic carbon (DOC) and b) dissolved inorganic carbon (DIC). The box of Panozzalacke (Panozza) is based on all samples collected across the entire monitoring period. In the ‚Donation' plot the surface water Fasangartenarm (Fasan) is included, which only contained surface water during donation periods.

3.6. Microbial abundance and activity

3.6.1. Total cell counts (TCC)

Total cell counts in all three groundwater sampling sites differed significantly from each other (LSMB – LSMI: $p < 0.001$, LSMB – LSMC: $p = 0.023$, LSMI – LSMC: $p < 0.001$).

A significant effect of donation on TCC was observed at LSMB ($W = 389$, $p < 0.001$), whereas no significant differences between donation and non-donation periods were detected at LSMI ($W = 234$, $p = 0.491$) or LSMC ($W = 143$, $p = 0.096$). During the donation periods, LSMB exhibited an average TCC of $2.16 \times 10^8 \pm 1.85 \times 10^8$ cells/L , which is approximately four times higher than during non-donation periods ($4.79 \times 10^7 \pm 2.26 \times 10^7$ cells/L; Figure 14a). LSMC exhibited an average TCC of $4.99 \times 10^7 \pm 2.48 \times 10^7$ cells/L, while LSMI showed the lowest mean values ($3.16 \times 10^7 \pm 9.34 \times 10^7$ cells/L), reflecting extremely high variability at this site. All three wells showed a peak in TCC on 20 July 2023.

Surface water exhibited significantly higher TCC values compared to groundwater ($W = 0$, $p < 0.001$). Mean concentrations were higher in the Panozzalacke ($4.25 \times 10^9 \pm 1.72 \times 10^9$ cells/L) than in the Fasangartenarm ($3.13 \times 10^9 \pm 5.62 \times 10^8$ cells/L), although this difference was not statistically significant ($W = 46$, $p = 0.157$). Both LSMB and Panozzalacke showed a seasonal trend, with the lowest values occurring between January and April. In the Panozzalacke, TCC was also significantly higher during donation periods compared to periods without donation, i.e. $5.203 \times 10^9 \pm 1.65 \times 10^9$ cells/L vs. $3.168 \times 10^9 \pm 1.08 \times 10^9$ cells/L; ($t = 2.96$, $p = 0.01$).

3.6.2. Microbial activity (intracellular ATP)

LSMI differed significantly from the other two groundwater sites ($p < 0.001$), whereas no significant difference was observed between LSMB and LSMC ($p = 0.899$). Only LSMB was significantly affected by the donation ($W = 391$, $p < 0.001$), while LSMI ($W = 279$, $p = 0.108$) and LSMC ($W = 257$, $p = 0.112$) exhibited no significant effect (Figure 14b). During donation periods, LSMB exhibited average intracellular ATP (iATP) concentrations approximately eight times higher than during non-donation periods (32.6 ± 24.8 pM vs. 4.72 ± 6.5 pM). LSMI also showed elevated iATP values during the 2023 donation period, although this increase was not statistically significant. LSMC showed average concentrations of 17.8 ± 151 pM, reflecting extreme variability, while LSMI showed the lowest mean values (4.39 ± 12.1 pM). All three wells reached their maximum iATP concentrations on 21 September 2023 (LSMB: 79.7 pM;

LSMI: 45.2 pM; LSMC: 151 pM). Surface water iATP concentrations were significantly higher than in groundwater (W = 10, $p < 0.001$). Within surface waters, Panozzalacke exhibited significantly higher ATP concentrations than the Fasangartenarm (W = 32, p = 0.004), with mean values of 2599 ± 3067 pM compared to 568 ± 396 pM in the Fasangartenarm.

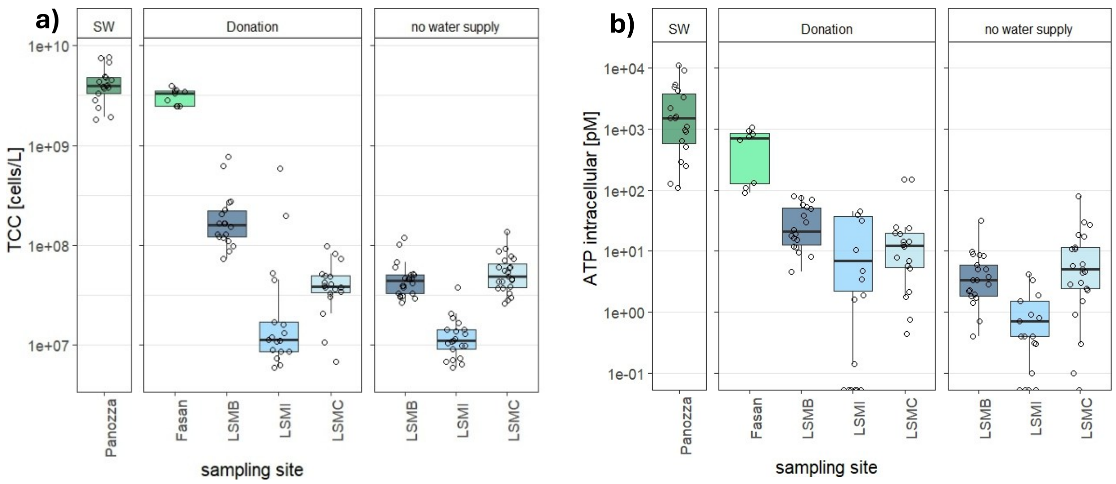

Figure 14. Boxplots of a) total cell counts (TCC) and b) intracellular ATP. The box of Panozzalacke (Panozza) is based on all samples collected across the entire monitoring period. In the ‚Donation' plot the surface water Fasangartenarm (Fasan) is included, which only contained surface water during donation periods. The y-axis of both plots is displayed in a logarithmic scale.

3.7. Greenhouse gases

3.7.1. Methane (CH_4)

Overall samples from the three groundwater wells did not differ in their CH_4 concentrations ($\chi^2 = 5.11$, df = 2, p = 0.078), although their temporal patterns and concentration ranges varied. All groundwater wells showed seasonal dynamics. At LSMB, concentrations increased during the summer months, ranging from 18.8 to 51.1 µM. Winter and spring values remained very low (0.01 – 1.12 µM). This seasonal pattern was more pronounced in 2023 compared to 2024. LSMC exhibited a similar seasonal trend, but with a slight delay (Figure 15a). The lowest values in LSMC occurred between April and June 2023 (0.01 – 1.20 µM) and again in May 2024. Highest concentrations in LSMC (15.2 – 27.1 µM) were measured in late summer and autumn in both years. In contrast LSMI showed the opposite pattern to LSMB with highest concentrations during autumn and winter (4.33 – 6.93 µM) and decreased during summer (Figure 15a). Overall the lowest CH_4 concentrations in groundwater were measured in well LSMI.

Surface water donation had a significant effect on CH_4 concentrations at LSMB ($W = 411$, $p < 0.001$), where values increased during donation (32.2 ± 24.7 µM), compared to periods without surface water supply (1.44 ± 1.66 µM; Figure 16a). No significant effect of donation on LSMC ($W = 226$, $p = 0.573$) or LSMI ($W = 128$, $p = 0.067$) was detected. Surface water bodies Panozzalacke and Fasangartenarm differed significantly from each other ($W = 97$, $p = 0.001$). The Panozzalacke exhibited lower and less variable CH_4 concentrations (0.30 ± 0.42 µM) compared to the Fasangartenarm (4.43 ± 5.53 µM). The Panozzalacke also differed significantly from all three groundwater wells (LSMB: $p < 0.001$; LSMI: $p = 0.004$; LSMC: $p < 0.001$), while the Fasangartenarm did not differ significantly from any of the groundwater sampling sites ($p = 1$).

3.7.2. Carbon dioxide (CO_2)

Significant differences in CO_2 concentrations were observed among the groundwater monitoring points. LSMI differed significantly from both LSMB and LSMC ($p < 0.001$), whereas LSMB and LSMC did not differ significantly from each other ($p = 0.30$). Among the three wells, LSMC exhibited the highest mean CO_2 concentrations (626 ± 37 µM), while LSMI showed the lowest (519 ± 40.8 µM). In LSMB average concentrations of 592 ± 107 µM were measured. No significant effect of the donation periods was detected at any of the groundwater sites (LSMB: $W = 248$, $p = 0.423$; LSMI: $W = 267.5$, $p = 0.05$; LSMC: $W = 249$, $p = 0.239$). Both LSMB and LSMC showed a slight increase in CO_2 concentrations during the 2023 donation phase. In 2024, concentrations initially decreased during the first half of the donation phase, followed by an increase in the second half (Figure 15b). Groundwater CO_2 concentrations differed significantly from those in surface water ($W = 2702$, $p < 0.001$). The two surface water bodies also differed significantly from each other ($W = 98$, $p = 0.003$), with Panozzalacke showing lower concentrations (165 ± 83.3 µM) compared to the Fasangartenarm (258 ± 117 µM).

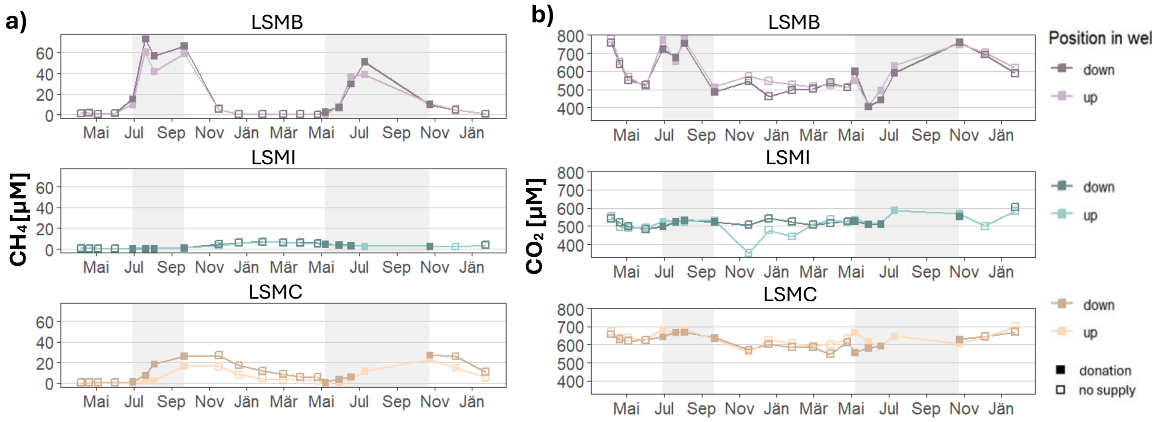

Figure 15. a) Methane (CH_4) and b) carbon dioxide(CO_2) over time at the three groundwater wells showing measurements at both well positions (up and down). Filled points and grey background indicate periods of donation.

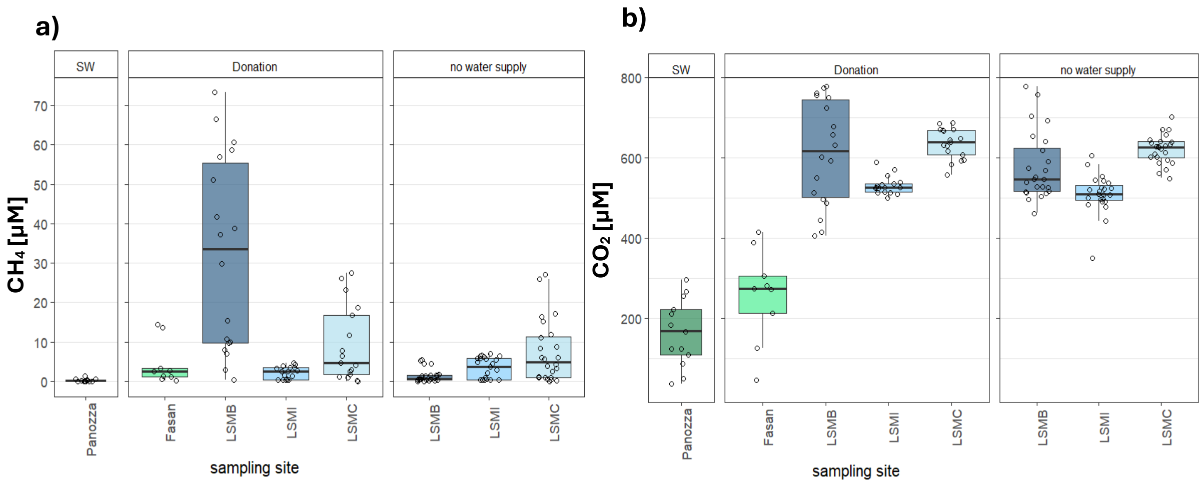

Figure 16. Boxplots of a) methane (CH_4) and b) carbon dioxide (CO_2). The box of Panozzalacke (Panozza) is based on all samples collected across the entire monitoring period. In the ‚Donation' plot the surface water Fasangartenarm (Fasan) is included, which only contained surface water during donation periods.

3.8. Fauna

3.8.1. Distribution and abundance of stygobiont, stygophile and stygoxene taxonomic groups

Over the entire monitoring period, a total of 557 individuals were collected across all three sampling sites. Well LSMC contained the highest number of individuals, followed by LSMB and LSMI.

In LSMB, 125 individuals were collected, of which 92% were stygobiont and 8% were stygoxene, with no stygophile individuals. In LSMC, a total of 361 individuals was recorded, consisting of 95.56 % stygobiont, 0.27% stygophile, and 4.16% stygoxene individuals. LSMI showed the lowest number of individuals, with a total of 71 individuals collected, of which 56.34% were stygobiont and 43.66% stygoxene; again no stygophile individuals were found (Figure 17).

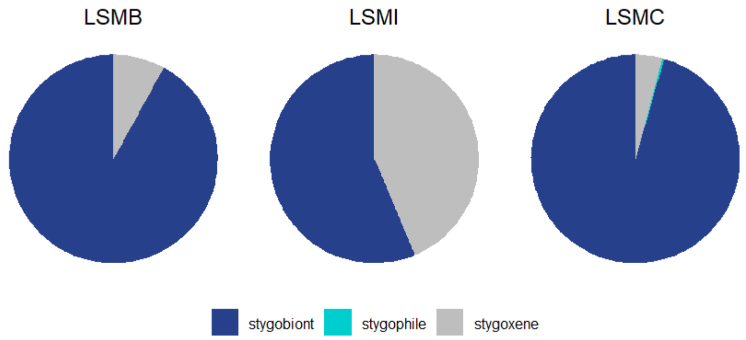

Figure 17 Proportional occurrence of stygobiont, stygophile, and stygoxene taxonomic groups, based on all individuals collected during the monitoring period.

During donation periods, the proportion of stygobiont individuals was slightly higher in LSMB, with 75 individuals recorded (96% stygobiont, 4% stygoxene) compared to 50 individuals outside donation periods (86% stygobiont, 14% stygoxene). In LSMI, only 20 individuals were found during donation periods (30% stygobiont, 70% stygoxene), while 51 individuals were collected outside donation periods (66.67% stygobiont, 33.33% stygoxene). In LSMC the proportion of stygobiont individuals was also slightly higher during donation periods, 199 individuals were recorded during donation (99% stygobiont, 0.5% stygophile, 0.5% stygoxene) and 162 individuals outside donation periods (91.36 % stygobiont, 8.64% stygoxene). No stygophile taxa were detected in LSMB or LSMI.

For subsequent analyses, only stygobiont and stygophile taxa were considered. Across the entire monitoring period 501 stygobiont and stygophile individuals were recorded in total: 115 in

LSMB, 346 in LSMC, and 40 in LSMI. Eleven different taxonomic groups were identified in LSMC, 8 in LSMB and 7 in LSMI. Considering donation periods separately, a total of 6 different taxonomic groups were found in LSMB during both donation periods (7 outside donation), 3 in LSMI during donation periods (6 outside donation) and 7 each in LSMC both during and outside donation periods.

3.8.2. Absolute Abundance and taxonomic composition

Absolute abundances of all taxonomic groups across the three sampling sites, grouped by donation or periods without donation are summarized in Table 4. Across the three wells LSMB, LSMI and LSMC the taxonomic composition showed differences in terms of presence. In general Cyclopoida showed the highest numbers in all three wells. Plathelminthes were detected only in LSMC, with a single individual recorded during one of the donation periods. Oligochaeta were present in all three wells, in LSMB only abundant during donation and more abundant outside donation periods in LSMI and LSMC. Gastropoda occurred only in LSMB and LSMC, with higher abundance during donation periods in both. Nematodes were found in all three wells, being abundant only during periods without surface water supply. Ostracods were also found in all three wells. While LSMB and LSMC showed higher numbers of Ostracods during donation, LSMI was found exclusively outside donation periods. Cyclopoida were present in all wells too, showing much higher abundance during periods without surface water donation in LSMI, slightly higher abundance during donation in LSMB and approximately twice as many individuals during donation periods in LSMC. Amphipoda were found in all three wells, being more abundant during donation periods in LSMB and only one individual occurred in LSMC outside donation periods. Isopoda were more abundant during donation in LSMB, more abundant outside donation in LSMC, and absent from LSMI. Bathynellaceae were represented by a single individual in LSMI outside donation, by one individual during donation in LSMC and were not detected in LSMB. Acari were equally abundant during and outside donation in LSMI, occurred only outside donation in LSMB, and only during donation in LSMC. Chironomidae larvae were observed only in LSMC, with a single individual recorded during donation.

Taxonomic group	LSMB (donation)	LSMB (no donation)	LSMI (donation)	LSMI (no donation)	LSMC (donation)	LMSC (no donation)
Plathelminthes	-	-	-	-	1	-
Oligochaeta	2	-	1	3	24	48
Polichaeta	-	-	-	-	-	-
Gastropoda	8	1	-	-	19	11
Nematodes	-	2	-	2	-	3
Tardigrada	-	-	-	-	-	-
Ostracods	5	2	-	3	40	18
Cyclopoida	43	34	1	21	104	50
Harpaticoida	-	-	-	-	-	-
Diplostraca	-	-	-	-	-	-
Amphipoda	4	1	1	1	-	1
Isopoda	10	1	-	-	2	10
Bathynellaceae	-	-	-	1	1	-
Acari	-	2	3	3	6	-
Plecoptera_Larvae	-	-	-	-	-	-
Chironomidae_Larvae	-	-	-	-	1	-

Table 3. Number of individuals recorded for each taxonomic group at the three groundwater monitoring sites, shown separately for donation and non-donation periods.

In terms of absolute abundance all monitoring wells differed significantly from each other (LSMB–LSMI: $p = 0.034$; LSMB–LSMC: $p = 0.002$), with the strongest difference observed between LSMC and LSMI ($p < 0.001$). No significant differences in absolute abundance between donation and periods without donation were observed at LSMI ($W = 28$, $p = 0.098$) or LSMC ($W = 68.5$, $p = 0.158$). In contrast, LSMB exhibited significantly higher abundances during donation periods compared to non-donation periods ($W = 76$, $p = 0.047$). At LSMB very low absolute abundance was observed at the beginning of the monitoring period, with only two individuals recorded on 6 April 2023, followed by three samplings with no individuals detected. During the first donation period, absolute abundance increased to eight individuals and subsequently peaked at eleven individuals, followed by a decline afterwards. Outside donation periods an increase was recorded on 19 December 2023, with 17 individuals, followed by an immediate decline. During the 2024 donation period, abundance increased again, reaching a maximum of 17 individuals, after which it slightly decreased.

LSMC exhibited the highest absolute abundances among all three sampling sites. At the first sampling 23 individuals were recorded. From late April 2023 to March 2024, absolute abundance ranged between 8 and 12 individuals per sampling event, with a decrease to three individuals in July 2023. The highest abundance at LSMC occurred during the donation period in May and June 2024 (maximum 44 individuals). Subsequently abundance declines to seven individuals in December 2024, followed by an increase in January 2025 (33 individuals). LSMI showed the lowest absolute abundance and the highest number of sampling events with no individuals detected. When individuals were present, absolute abundances typically ranged between one and three individuals per sample. Notable increases for this well were observed in February 2024 (15 individuals) and April 2024 (7 individuals; Figure 18).

Absolute abundance across the three groundwater sampling sites correlated significantly with several parameters. Significant positive correlations were observed with DO ($\rho = 0.41$, $p = 0.001$), temperature ($\rho = 0.487$, $p < 0.001$), SiO_4^{4-} ($\rho = 0.61$, $p < 0.001$), CO_2 ($\rho = 0.393$, $p = 0.002$), CH_4 ($\rho = 0.496$, $p < 0.001$) and TCC ($\rho = 0.403$, $p = 0.002$). Significant negative correlations were detected with EC ($\rho = -0.35$, $p = 0.006$), PO_4^{3-} ($\rho = -0.592$, $p < 0.001$), SO_4^{2-} ($\rho = -0.648$, $p < 0.001$), Mg^{2+} ($\rho = -0.519$, $p < 0.001$), Na^+ ($\rho = -0.281$, $p = 0.029$), Cl^- ($\rho = -0.382$, $p = 0.003$) and Fe ($\rho = -0.382$, $p = 0.003$).

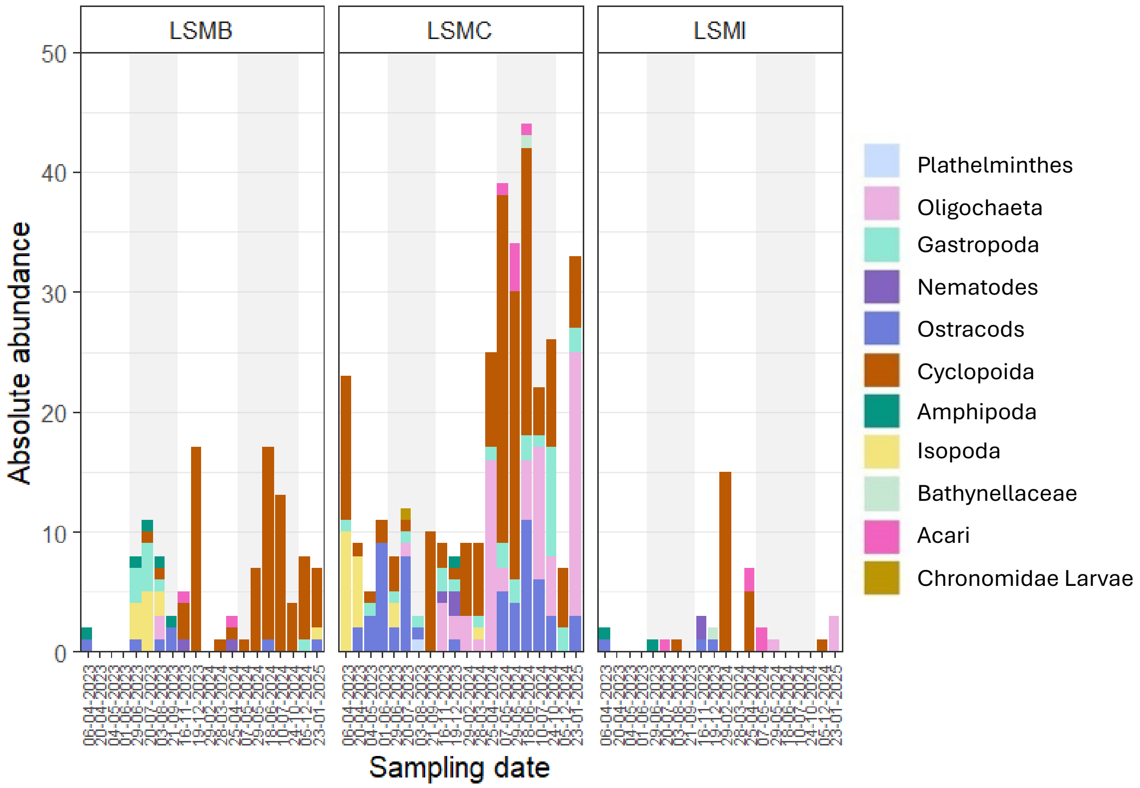

Figure 18. Absolute abundance and taxonomic composition of groundwater fauna at the sampling sites LSMB, LSMI and LSMC across the entire sampling period. Each bar represents one sampling event. Grey backgrounds indicate donation periods.

At LSMB multiple taxonomic groups co-occurred regularly during the early phase of monitoring. From September 2023 onwards, Cyclopoida increasingly dominated, despite being rare at the beginning of the sampling. This dominance became particularly evident during the donation period in 2024, when Cyclopoida abundances increased markedly. Gastropoda and Isopoda occurred more frequently during the donation period in 2023, followed by a phase in which Isopoda were absent and reappeared only once at the final sampling date 23 January 2025. Oligochaeta were recorded exclusively in August 2023. Amphipoda were no longer detected after September 2023 and a similar pattern was observed for Gastropoda and Isopoda, which only occurred occasionally towards the end of the monitoring period.

LSMI showed the lowest fauna presence compared to LSMB and LSMC. Many samples contained no individuals and simultaneous occurences of multiple taxonomic groups were rare. A peak was observed at 29 February 2024, consisting exclusively of Cyclopoida. Apart from this event abundances remained consistently low throughout the monitoring period.

LSMC exhibited the highest overall abundance among the three groundwater sampling sites. Ostracoda occurred most frequently from April/May to July. An increase of Oligochaeta was observed from late April 2024 onwards. Cyclopoida showed an increase during the donation period in 2024 together with elevated abundances of Oligochaeta and Ostracoda and declining abundances afterwards. A similar less pronounced pattern was observed at LSMB. Acari were detected exclusively during the summer months of 2024. Gastropoda were present in low numbers in nearly every sample and occurred more frequently towards the end of the second donation period in October 2025. Plathelminthes, Amphipoda, Chironomidae larvae and Bathynellaceae were recorded only at isolated sampling dates and always as single individuals (Plathelminthes on 3 August 2023, Amphipoda on 19 December 2023, Chironomidae larvae on 20 July 2023, Bathynellaceae on 18 June 2024). Isopoda were mainly recorded at the beginning of the monitoring period and were only detected again at two later sampling dates (29 June 2023 and 28 March 2024). Overall, LSMC showed a higher co-occurrence of multiple taxa compared to the other sites. Nematodes were detected nearly simultaneously at all three sampling sites in November 2023. At LSMB they were additionally recorded once more in April 2024 (Figure 18).

3.8.3. Relative Abundance

Considering all samples from the three groundwater wells over the entire monitoring period, Cyclopoida constituted the largest proportion of individuals at all wells, accounting for 67% at LSMB, 55% at LSMI and 44.5% at LSMC.
At LSMC, Oligochaeta represented the second most abundant taxonomic group (20.8%), followed by Ostracoda (16.8%), Gastropoda (8.67%), Isopoda (5.49%) and Acari (1.7%). The least abundant groups at LSMC over the entire monitoring period were Amphipoda, Bathynellaceae and Chironomidae larvae (each 0.29%), while Nematodes accounted for 0.9%.

At LSMB, Gastropoda showed a similarly high proportion (7.82%) compared to LSMC. Isopoda were slightly more abundant at LSMB (9.56%) than at LSMC. In addition, Ostracoda (6.09%) and Amphipoda (4.35%) were present at LSMB. Oligochaeta, Nematodes and Acari each contributed equally, with proportions of 1.74%.
At LSMI Acari represented the second most abundant group (15%), followed by Oligochaeta (10%), Ostracoda (7.5%) ,Amphipoda and Nematodes (each 5%). Bathynellaceae were the least abundant at LSMI, with a proportion of 2.5% (Figure 19).

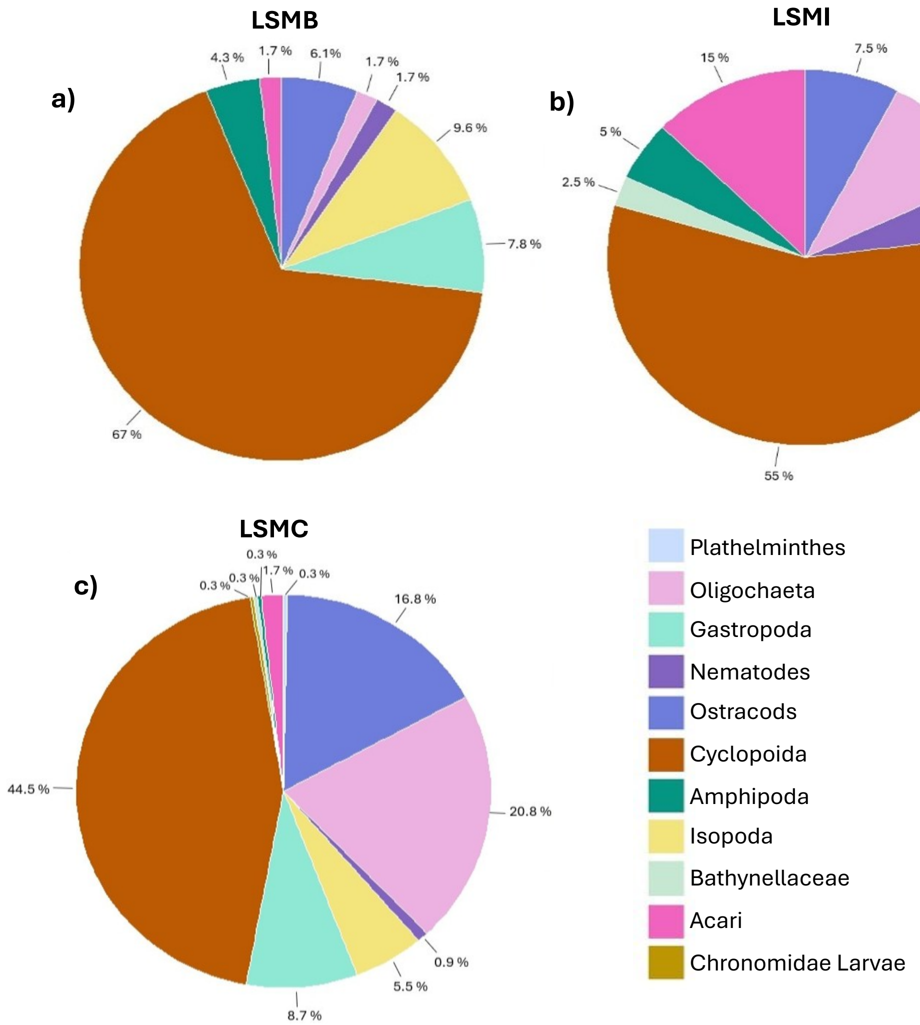

Figure 19. Pie charts showing the relative abundances of the recorded taxonomic groups at the three groundwater sampling sites LSMB, LSMI, and LSMC. For each sampling site, proportions are based on all individuals collected over the entire monitoring period.

The taxonomic group composition differed considerably between the first and second donation periods and also varied across periods without donation. Figure 20 presents the relative abundances of taxonomic groups during these phases. The period „no donation 2023" covers 6 April 2023 to 1 June 2023, „donation 2023" represents the first donation phase from 29 June

2023 to 21 September 2023, „no donation 2023/2024" covers 16 November 2023 to 25 April 2024, „donation 2024" covers the second donation phase from 7 May 2024 to 24 October 2024 and „no donation 2024/2025" includes the final two sampling dates, 5 December 2024 and 23 January 2025.

During the „no donation 2023" phase, LSMB and LSMI showed relative abundances of 50% each for Ostracoda and Amphipoda. In LSMB the relative abundances between the two donation phases differed markedly. The highest proportions in LSMB during donation 2023 were from Gastropoda and Isopoda (33.3% each). Ostracoda and Amphipoda each contributed 13.3%, while Oligochaeta and Cyclopoida were present 6.7% each. In contrast during the second donation period in 2024 Cyclopoida dominated with 97.6%, Ostracoda accounted for 2.38% and the other taxonomic groups were absent. In LSMB a notable increase in Cyclopoida was also observed from autumn 2023 onwards with relative abundances ranging from 80% to 97.6%.

In LSMC, the two donation phases showed smaller differences in the distribution of taxonomic groups compared to LSMB. The proportion of Cyclopoida was slightly higher during the donation period 2024 (54.5%) than in the donation period 2023 (42.4%). The relative abundance of Oligochaeta also increased during the 2024 donation phase (13.4%) compared to 2023 (0.33%). In contrast, the proportion of Ostracoda was lower in 2024 (17.6%) than in 2023 (33.3%). Similar to LSMB, Isopoda were present in LSMC only during the first donation phase. Bathynellaceae accounted for 0.61% in LSMC during the donation phase 2024, whereas they were absent in the 2023 donation phase. Gastropoda were consistently present in LSMC throughout the entire period, with relative abundances ranging from 4.17% to 10%. Oligochaeta exhibited higher relative abundances during the non-donation periods 2024 and 2025 in LSMC, compared to the beginning of the sampling.

LSMI showed the most variable relative abundances throughout the monitoring period. During the „no donation 2023/2024" Cyclopoida dominated clearly with a relative abundance of 71.4%, while in the donation phase 2024 Acari (66.7%) and during the „no donation 2024/25" Oligochaeta (75%) reached very high relative abundances. It is important to note that the LSMI samples contained fewer individuals than those from the other two sampling sites.

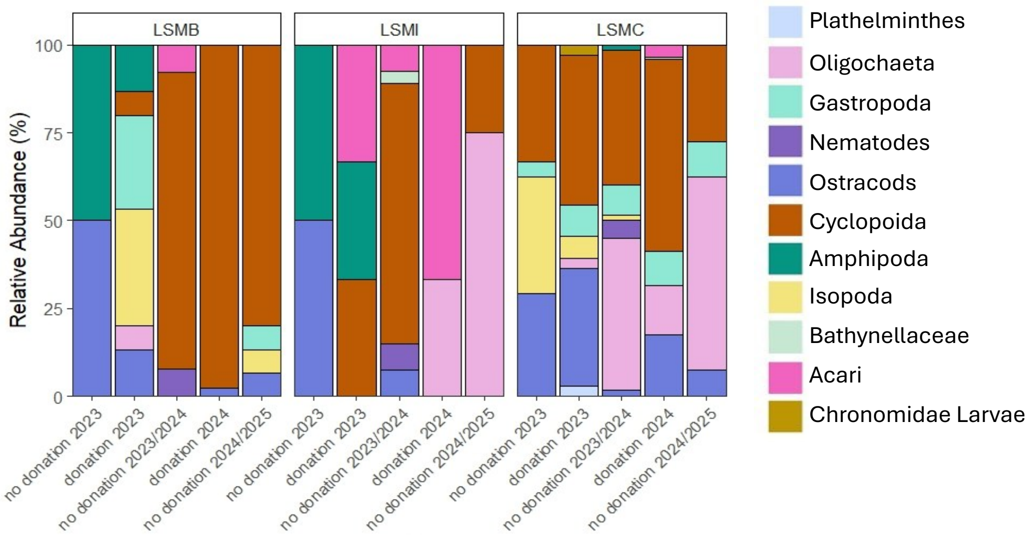

Figure 20. Relative abundance (%) of LSMB, LSMI, and LSMC, separated by donation and non-donation periods.

3.8.4. Shannon Diversity

Shannon diversity in LSMC was significantly different from that in LSMB and LSMI (LSMB – LSMC $p = 0.002$, LSMC – LSMI $p < 0.001$), while LSMB and LSMI did not differ significantly from each other ($p = 0.056$). LSMC exhibited the highest average Shannon diversity (0.96 ± 0.37), followed by LSMB (0.43 ± 0.54) and LSMI with the lowest (0.13 ± 0.27; Figure 21).

In LSMB, there was no significant difference in Shannon diversity between donation and non-donation periods (without differentiating the two donation phases; $W = 58$, $p = 0.516$). However, it should be noted that the 2023 donation phase in LSMB differed significantly from the 2024 donation phase ($W = 20$, $p = 0.015$). During the donation 2023, Shannon diversity was higher on average (1.2 ± 0.45), whereas during the 2024 donation, it was considerably lower (0.05 ± 0.1). During the non-donation periods, the average Shannon diversity was 0.74 ± 0.4. The highest Shannon diversity observed in LSMB was 1.73 on 03 August 2023. In LSMC, there was also no significant difference in Shannon diversity between donation and non-donation periods ($W = 68$, $p = 0.175$). Unlike LSMB, no difference was observed between the 2023 and 2024 donation phases ($W = 9$, $p = 0.905$). The average Shannon diversity over the entire period was 0.96.

In LSMI, the difference in Shannon diversity between donation and non-donation periods was also not significant ($W = 31.5$, $p = 0.057$). Shannon diversity in LSMI was highest on 06 April

2023 and 19 December 2023 (0.69). During the donation phases, Shannon diversity remained consistently at 0, while during non-donation periods, the average was 0.24 ± 0.33. Both LSMB and LSMI recorded a Shannon diversity of 0 in multiple samples, whereas in LSMC this was observed only on 21 September 2023.

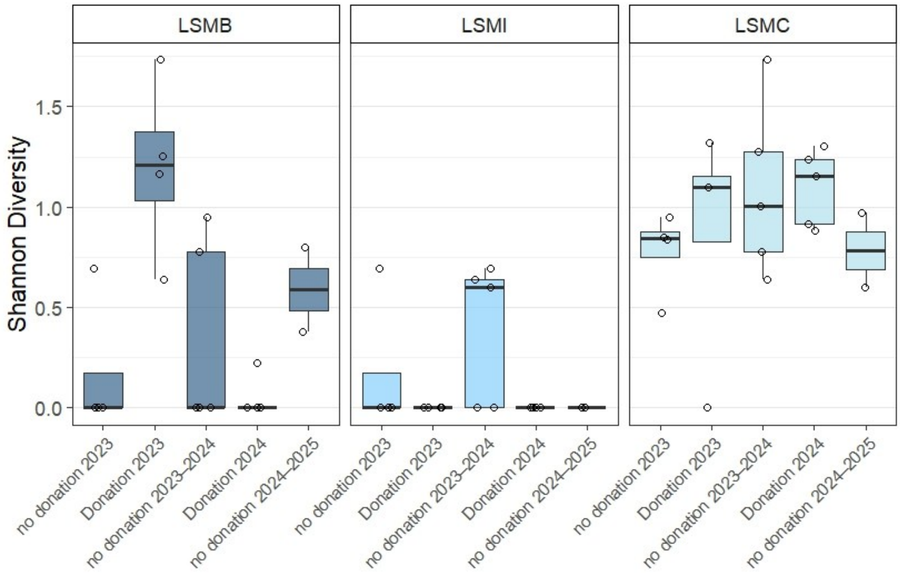

Figure 21. Shannon diversity at the three groundwater sampling sites (LSMB, LSMI, LSMC) during donation and non-donation periods.

3.8.5. Taxa richness

LSMC differed significantly from the other two sampling sites in terms of taxa richness, as observed for Shannon diversity (LSMC – LSMB: $p = 0.002$; LSMC – LSMI: $p < 0.001$). LSMB and LSMI did not differ significantly from each other, although the difference was close to significance ($p = 0.05$).

In LSMB, taxa richness did not differ significantly between donation and non-donation periods ($W = 67$, $p = 0.186$). However, a significant difference was observed between the 2023 and 2024 donation phases ($W = 20$, $p = 0.02$; Figure 22). The taxa richness during the 2023 donation was 4, but dropped to 1 during the 2024 donation. By comparison, the average taxa richness during non-donation periods was 1.36 ± 0.83. The highest taxa richness was recorded on 03 August 2023, with a value of 6. In LSMC, taxa richness did also not differ significantly between donation and non-donation periods ($t = 1.25$, $df = 18$, $p = 0.228$). LSMC exhibited the highest average taxa richness across all three sampling sites, with a mean of 3.6 ± 1.31. The maximum taxa richness in LSMC was 6, observed on 19 December 2023 and 18 June 2023. LSMI showed the lowest average taxa richness of all three sites, with a mean of 0.85. The maximum taxa richness observed in LSMI was 2. No significant difference was found between donation and non-donation periods in LSMI (W = 31, p = 0.14).

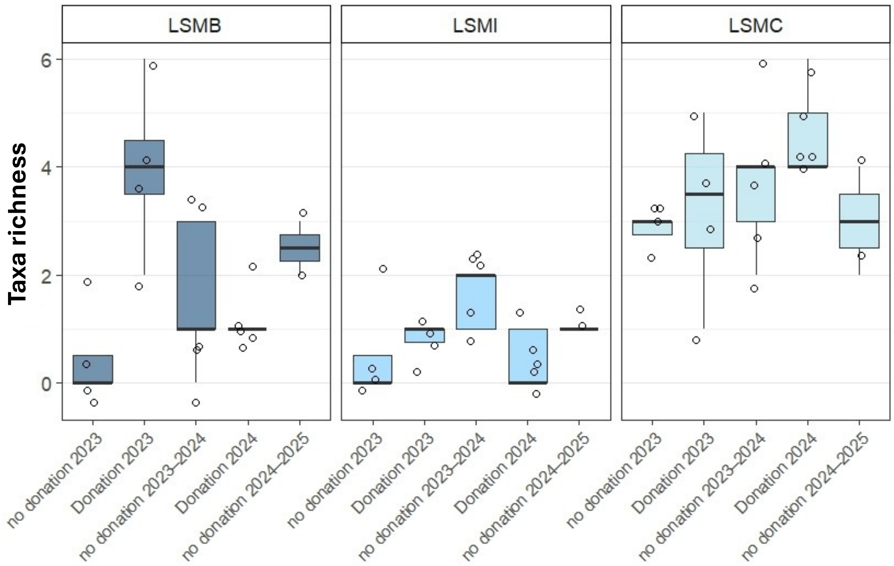

Figure 22. Species richness at the three groundwater sampling sites (LSMB, LSMI, LSMC) during donation and non-donation phases.

3.9. Phase and site-specific correlation patterns during donation periods and periods without donation

Previous analyses indicated that surface water donation primarily affected well LSMB. Therefore, additional correlation analyses were performed separately for LSMB and for the combined dataset of LSMI and LSMC. While LSMB exhibited phase-dependent changes in correlation patterns, correlations at LSMI and LSMC were comparatively stable between donation and non-donation periods (Figure 23).

In LSMB, DO exhibited a strong negative correlation with NH_4^+ exclusively during donation periods. A comparable negative relationship was also observed at LSMI and LSMC. Likewise, the correlation between DO and iATP was strongly negative in LSMB only during donation, whereas it persisted with comparable strength across both phases at LSMI and LSMC.

Temperature-related patterns further emphasized the distinct behavior of LSMB. A strong negative correlation between temperature and SO_4^{2-} was observed in LSMB during non-donation periods only, while this relationship remained consistent across phases at LSMI and LSMC. In contrast, strong positive correlations between temperature and Mn^{2+}, PO_4^{3-}, and CH_4 occurred exclusively during donation in LSMB, at the other sites these relationships were either absent or phase-independent.

Also DOC dynamics differed between the wells. DOC exhibited a strong positive correlation with NO_3^- in LSMB exclusively during non-donation periods; no corresponding relationship was observed at LSMI and LSMC. The negative correlation between DOC and SO_4^{2-} was more pronounced during donation in LSMB but generally consistent with the patterns observed at the other wells. DOC and Fe^{2+} were strongly positively correlated in LSMB during donation, while a moderate negative relationship was observed at LSMI and LSMC during the same phase. Moderate positive correlations between DOC and P total were also restricted to donation periods in LSMB. The correlations between DOC and CH_4 as well as DOC and CO_2 were more strongly positive in LSMB during non-donation periods compared to donation phases. At LSMI and LSMC, these relationships exhibited comparable moderate strengths across phases.

Nitrate was strongly positively correlated with Mn^{2+} and CO_2 in LSMB exclusively during non-donation periods, while no significant relationships were observed at LSMI and LSMC. SO_4^{2-} exhibited very strong negative correlations with Fe^{2+}, PO_4^{3-} and P total in LSMB during periods without donation. In contrast, SO_4^{2-} at LSMI and LSMC was strongly positively correlated with Fe^{2+} during donation and its relationship with PO_4^{3-} remained comparatively stable across phases. During donation, SO_4^{2-} was very strongly negatively correlated with CO_2 and CH_4 in LSMB, while correlation strengths remained comparatively stable at the other two wells. NH_4^+ and HS^- were very strongly positively correlated in LSMB exclusively during donation periods, this relationship was only moderate at LSMI and LSMC. SiO_4^{4-} was strongly negatively correlated with CO_2 in LSMB during donation. Outside donation periods, HS^- exhibited strong positive correlations with Mn^{2+} and PO_4^{3-} in LSMB, as well as a moderate positive correlation with CH_4. These relationships were absent or only weakly expressed at LSMI and LSMC. Strong negative correlations between iATP and both NH_4^+ and HS^- were likewise restricted to donation periods in LSMB, while only moderate negative relationships were observed at the other sites.

Ferrous iron and Mn^{2+} were very strongly negatively correlated in LSMB exclusively during donation periods, while this relationship was only moderate at LSMI and LSMC. The correlation between Fe^{2+} and P total was more strongly negative in LSMB during non-donation periods, whereas stronger positive relationships were observed at LSMI and LSMC outside donation. Fe^{2+} and CH_4 were more strongly negatively correlated in LSMB during non-donation periods, while no significant relationship was observed at the other sites. Mn^{2+} exhibited a very strong positive correlation with CO_2 and a strong positive correlation with TCC in LSMB exclusively during non-donation periods; at the other sampling sites these relationships were only moderate.

Phosphate and P total were more strongly positively correlated during donation and PO_4^{3-} showed a moderate positive correlation with CO_2 during non-donation. A strong positive PO_4^{3-}–CH_4 correlation occurred exclusively during donation in LSMB. CO_2 and CH_4 were very strongly positively correlated during donation in LSMB, whereas no significant relationship was observed at LSMI and LSMC. Similarly, strong positive correlations between CH_4 and TCC as well as between TCC and iATP were restricted to donation periods in LSMB; at the other wells, these relationships were weaker or absent.

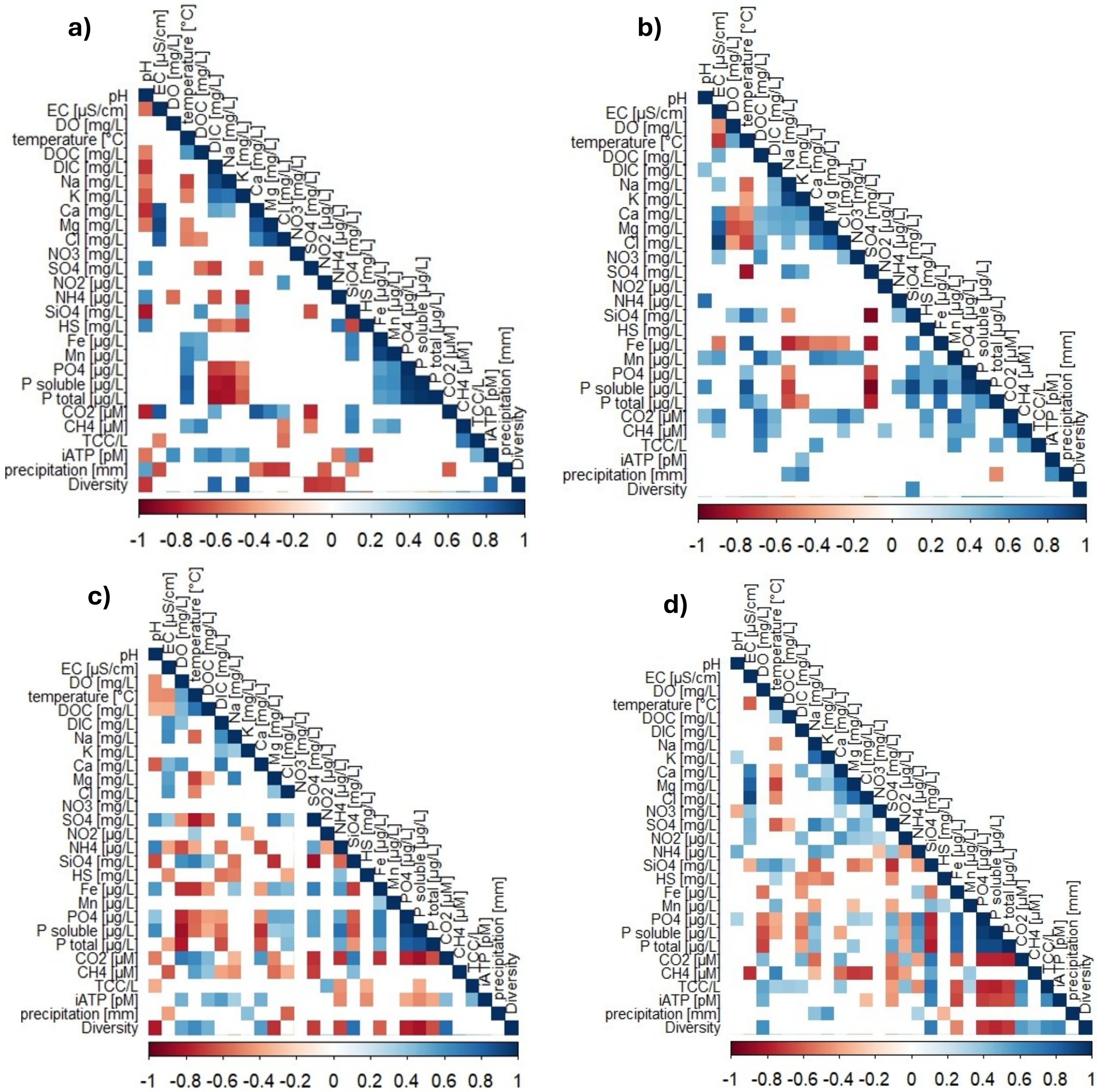

Figure 23. Spearman correlation matrices of measured and analysed parameters during donation and during periods without surface water donation. The matrices show a) LSMB during donation, b) LSMB without donation, c) LSMI and LSMC during donation and d) LSMI and LSMC without donation. Color intensity represents Spearman's rank correlation coefficients (ρ), with blue indicating positive correlations and red indicating negative correlations.

4 Discussion

The aim of this thesis was to investigate the effects of surface water donation in the Upper Lobau via the New Danube, Panozzalacke and Fasangartenarm on groundwater quality as well as microbiological and faunistic pattern at three selected sampling sites LSMB, LSMI, and LSMC. To address this issue onsite environmental parameters, major ions, nutrients, microbial biomass and activity and invertebrate fauna composition were analyzed.

4.1. Groundwater level response to surface water donation

As expected surface water donation led to a significant increase in groundwater levels at all three sampling sites. LSMB, which is located closest to the surface water, exhibited the most and fastest pronounced increase in groundwater levels throughout the entire sampling period, reflecting its close connection to the surface water system. Groundwater levels increased similarly with some delay at LSMB and LSMC, with LSMC being the most distant well from the surface water bodies. This pattern corresponds to the typical distance-dependent recharge response described by Jin et al. (2024), where groundwater level increases are generally strongest near the recharge source. From LSMB to LSMC a difference in hydraulic head (gw level a.s.l.) of 63 to 145 cm was observed. According to Parlov et al. (2019) recharge dynamics are modulated by aquifer heterogeneities, i.e. the thickness of the unsaturated zone and soil permeability, which can lead to stronger groundwater level increases at sites more distant from surface water bodies than those closer to it. Also precipitation has an impact to groundwater levels via local groundwater recharge. In our case, the correlation between groundwater levels and recent precipitation was weak and non-significant, indicating that short-term rainfall events had little influence on groundwater levels during the monitoring period. This suggests that the observed changes in groundwater levels were primarily driven by groundwater recharge from surface water from the oxbow channel Fasangartenarm, rather than by rainfall. This observation that the groundwater level rises due to infiltration and the little or no response to precipitation is consistent with previous studies (Yin et al., 2025; Parlov et al., 2019). It is important to note that no groundwater sampling took place during or shortly after the flood events in early September 2024. Since the first sampling after these events took place at the end of October 2024, the available data do not allow a clear assessment of possible short term groundwater responses to flooding or heavy rainfall.

4.2. Effects of surface water donation at LSMB

Apart from the groundwater level, which was affected by the donation at all three sampling sites, the donation had a noticeable effect on groundwater quality only at LSMB, where several parameters responded to the donation, which was not the case in LSMI and LSMC. This was likely because LSMB is the well closest to the surface water. As reported by Marmonier et al. (2023), aquatic subterranean habitats with closer connectivity to surface water generally exhibit increased temporal variability, with more pronounced fluctuations in nutrients, organic matter and dissolved oxygen. The response observed at LSMB mostly aligns with these findings, highlighting how surface water inputs can rapidly change certain hydrochemical and microbial parameters in connected groundwater zones. Electrical conductivity (EC) was lower during the donation in LSMB due to dilution, as EC in the surface water of Fasangartenarm was lower compared to the groundwater. The decrease in EC in Panozzalacke during the donation further suggests that the EC of the Danube is lower than that of Panozzalacke and that the donation also diluted the surface water of Panozzalacke. Similarly, the lower magnesium concentration observed at LSMB during the donation indicates dilution with surface water, since magnesium levels in the surface water were also lower than in the groundwater compared to periods without donation. These findings are consistent with previous studies, which reported decreases in major ion concentrations and changed hydrochemical conditions during recharge due to the lower ion content of surface water (Jin et al., 2024; Li et al., 2023; Jiang et al., 2025a). Groundwater temperature at LSMB was significantly higher during donation periods, as the donation took place in spring, summer and autumn, infiltrating surface water warmer than groundwater and reflecting seasonal trends due to the proximity of the well LSMB to the surface water. As shown in modeling studies by Epting et al. (2022), such infiltration can significantly increase groundwater temperature and pumping for drinking water extraction can cause local cooling in groundwater. Accordingly, LSMC which is located close to the drinking water production well exhibited lower groundwater temperatures than LSMB. Nitrite concentrations at LSMB were significantly higher during donation. This indicates active denitrification. At our sampling sites, dissolved oxygen concentrations were consistently low, particularly at LSMB and LSMI, indicating that the system is generally oxygen-limited. Jiang et al. (2025a) reported that ecological water replenishment enhances redox-driven microbial activity, stimulating denitrifying bacteria and nitrogen transformations. In this context, the elevated nitrite concentrations at LSMB can be attributed to incomplete nitrate reduction under hypoxic and anoxic conditions (Griebler & Mösslacher, 2003). Nitrate reduction becomes energetically favorable once oxygen is depleted (Rivett et al., 2008) and the presence of nitrite indicates that redox processes are still ongoing, providing evidence for active denitrification (Appelo & Postma, 2005; Kölle, 2017). The data suggest that incomplete denitrification occurs during surface water donation, consistent with the findings of Jiang et al. (2025a). DOC concentrations at LSMB were also significantly higher during donation periods. In groundwater, DOC originates primarily from external sources, such as input from surface water or transport through the subsurface (Griebler & Mösslacher, 2003; Marmonier et al., 2023; Schwoerbel & Brendelberger, 2022). Therefore, the observed increase in DOC during donation can be attributed to the infiltration of surface water from the Fasangartenarm. Furthermore, both the Fasangartenarm and the Panozzalacke contained higher amounts of organic material than the groundwater at LSMB, supporting this assumption. Sulfate (SO_4^{2-}) concentrations were significantly lower during the donation period at LSMB. Sulfate concentrations in the Fasangartenarm were higher than in LSMB, this provides evidence that sulfate reduction may have occurred. As sulfide concentrations in LSMB did not increase during the donation, sulfate reduction either took place within the sediments of Fasangartenarm, where the produced sulfide remained trapped and was not transported into the aquifer. This interpretation is consistent with Lee & Lee (2018), who demonstrated that infiltration of surface water during managed aquifer recharge stimulates microbial metabolism in both sediment and groundwater, leading to enhanced sulfate reduction. It is very likely that the sulfide produced reacted with ferrous iron originating from iron reduction forming insoluble FeS. At LSMB, total cell counts (TCC) were approximately four times higher during donation compared to periods without surface water supply. This observation is consistent with Fillinger et al. (2021), who reported a tenfold increase in microbial cell numbers within just a few days following river infiltration into a shallow aquifer. While Fillinger et al. (2021) studied direct river infiltration, in our case it involves surface water infiltration from an oxbow channel, but the microbial response is comparable. The increase could possibly be driven by the transport of microorganisms from the surface water into the groundwater (Marmonier et al., 2023). In addition, improved conditions for microbial growth during donation, particularly higher groundwater temperatures and DOC, likely enhanced microbial metabolic rates and growth as biochemical reaction rates generally increase with temperature (Chapelle, 1993). Changes in water chemistry caused by the donation, particularly lower ionic strength and altered cation composition in the infiltrating water may also enhance microbial mobility by reducing electrostatic interactions between cells and sediment particles (Li et al., 2026), which could further contribute to the observed increase in TCC. Correspondingly, intracellular ATP concentrations were observed to increase up to eightfold higher during the donation in LSMB, reflecting the increased metabolic activity of the microbial community under these favorable conditions, like higher temperature (Griebler & Mösslacher, 2003; Schwoerbel & Brendelberger, 2022) and higher DOC concentration (Freeze & Cherry, 1979). Such temperature-driven increases in microbial abundance and activity are consistent with observations from urban groundwater systems, where higher summer temperatures were shown to result in elevated cell counts and increased iATP concentrations (Becher et al., 2025). Similarly, Riedel (2019) demonstrated that even moderate increases in groundwater temperature can intensify microbial processes, leading to enhanced microbial activity. Significantly elevated CH_4 concentrations were observed at LSMB during donation periods. Methane production in groundwater is typically associated with strictly anoxic conditions and results from microbial methanogenesis during the degradation of organic carbon (Chapelle, 1993). The elevated microbial activity during donation likely results in increased oxygen consumption during respiration (Aquilina et al., 2023; Griebler & Mösslacher, 2003; Freeze & Cherry, 1979), which promotes anoxic conditions favorable for methanogenic processes. Although CH_4 was present in the Fasangartenarm, concentrations in the surface water were substantially lower than those observed in groundwater at LSMB during donation, indicating that the observed methane enrichment cannot be attributed only to the surface water infiltration. In headwater wetlands, López Lloreda et al. (2024) demonstrated that CH_4 is predominantly produced in anoxic sediments. It is very likely that the increased CH_4 concentrations observed during surface water donation originates from the organic sediments of the Fasangartenarm. At LSMB, CO_2 concentrations did not increase significantly during donation periods, but they exhibited greater variability compared to periods without donation. This variability likely reflects a combination of factors, including the infiltration of DOC from surface water and the associated increase in microbial activity. Elevated microbial activity during donation, together with higher DOC availability, stimulates the mineralization of organic carbon, producing CO_2 in the process. The observed variability in CO_2 concentrations reflects the dynamic response of the microbial community to surface water donation, consistent with CO_2 serving as an indicator of microbial metabolic activity (Chapelle, 1993).

4.3. Changes in Redox-sensitive correlation structures during surface water donation

The correlation patterns observed during donation periods revealed differences between the sampling site LSMB, which was directly influenced by surface water donation and the wells LSMI and LSMC, where no immediate effects of the donation were observed. These differences reflect contrasting redox conditions at the sites. At LSMI and LSMC, correlations among key redox-sensitive parameters, such as dissolved oxygen, iron , manganese, sulfate, ammonium, phosphate, total phosphorus, sulfide, methane and carbon dioxide remained relatively stable across donation and non-donation phases. This stability indicates well-established redox conditions at these sites and suggests that surface water donation does not fundamentally change the dominant biogeochemical processes in LSMI and LSMC. During donation several strong correlations appear at LSMB that are not observed outside donation phases, including between DO and iATP, temperature and DOC, Fe^{2+} and Mn^{2+}, HS^- and iATP, NH_4^+ and iATP, iATP and DOC, SO_4^{2-} and CH_4, SO_4^{2-} and CO_2. The strengthened correlations between iATP, DO, and temperature during donation suggest that microbial activity responds to the changing environmental conditions due to donation. The strong positive correlation between Fe^{2+} and Mn^{2+} during donation, absent in non-donation periods, indicates that these metals are reduced synchronously under dynamically changing redox conditions induced by surface water infiltration. Organic matter degradation drives Fe^{2+} and Mn^{2+} reduction in alluvial aquifers (Appelo & Postma, 2005; Jiang et al., 2025b) and even if Fe^{2+} concentrations are not elevated during donation, the strong Fe^{2+}–Mn^{2+} correlation suggests early activation of Fe^{3+}- and Mn^{4+}-reduction. These observations highlight that short-term hydrological events, such as surface water donation, can significantly influence the transformation and transport of redox-sensitive metals in groundwater. They also align with Li et al. (2023), who demonstrated that DOC-rich recharge water stimulates microbial activity, drives Fe^{3+} and Mn^{4+} reduction and temporarily shifts redox conditions. DOC-rich recharge pulses stimulate microbial metabolism, initiating sequential redox reactions including iron and manganese reduction (Lee & Lee, 2018). These findings are further consistent with Feng et al. (2023) and Jiang et al. (2025a) who showed that organic matter introduced via surface water can directly influence redox reactions in groundwater. Some correlations that are strong during periods without donation weaken or disappear during donation periods, such as those between Fe^{2+} and CH_4, HS^- and Mn^{2+}, HS^- and PO_4^{3-}, Fe^{2+} and PO_4^{3-}, Fe^{2+} and P total, Mn^{2+} and CO_2, CO_2 and CH_4. Outside donation phases, LSMB is characterized by strong correlations among reduced species, indicating more reduced conditions in periods without surface water donation. These shifts demonstrate that LSMB represents a highly dynamic system in which biogeochemical relationships reorganize during donation.

4.4. Groundwater quality

Values of pH in all sampling sites, including surface waters, were within the drinking water range (6.5 – 9.5) and electrical conductivity did not exceed the threshold of 2500 µS/cm throughout the monitoring period (IS6). Across all groundwater samples, cation concentrations generally followed the order Ca^{2+}> Mg^{2+}> Na^{+} > K^{+}, while anions followed the order Cl^{-} > SO_4^{2-} > SiO_4 > HS^{-} > NO_3^{-}. Concentrations of major ions remained well below drinking water guideline values in all groundwater wells and surface waters. Calcium (Ca^{2+}, 400 mg/L), magnesium (Mg^{2+}, 150 mg/L), potassium (K^{+}, 50 mg/L), sodium (Na^{+}, 200 mg/L) and chloride (Cl^{-}, 200 mg/L) never exceeded their respective limits defined for drinking water quality (IS6). Sulfate (SO_4^{2-}, 250 mg/L) concentrations were consistently low, ranging from 2.9 to 25.7 mg/L (IS5: Republik Österreich, 2001). Water temperature in groundwater never exceeded the drinking water guideline of 25 °C, although surface waters occasionally surpassed this value during summer months (IS6). Nitrate (NO_3^{-}, 50 mg/L) and nitrite (NO_2^{-}, 0.10 mg/L) concentrations remained far below the drinking water limits in all groundwater wells throughout the monitoring period moreover, nitrate was frequently below the detection limit. Ammonium (NH_4^{+}, 0.50 mg/L) concentrations also remained below the guideline in groundwater at LSMC, LSMI and both surface waters during the entire monitoring period (0–264 µg/L). In LSMB, most measurements were below the limit, although a single peak of 632 µg/L was observed in the upper part of the well on 6 April 2023 (IS5: Republik Österreich, 2001). In contrast to the generally stable behavior of major ions and nutrients, redox-sensitive elements frequently exceeded drinking water guideline values. According to drinking water regulations, the guideline value for iron (Fe^{2+}, 200 µg/L) was continuously exceeded in groundwater at LSMB (271–3405 µg/L) and LSMI (1235–6361 µg/L), as well as in the Fasangartenarm surface water. In LSMC, Fe concentrations were partially below the guideline, particularly in the upper well sections at several sampling dates. Manganese (Mn^{2+}, 50 µg/L) concentrations exceeded the drinking water guideline in almost all groundwater wells and surface waters. The only period with Mn^{2+} concentrations below the guideline occurred in LSMC between May and August 2023, when values ranged from 0 to 32 µg/L (IS5: Republik Österreich, 2001). While surface water donation caused a dilution related decrease in magnesium concentrations and electrical conductivity at LSMB, this change cannot be interpreted as an improvement in groundwater quality, as major ions already complied with drinking water standards prior to donation.

4.5. Site specific groundwater conditions

Groundwater at LSMI differed most strongly from the groundwater at other two sites (LSMB, LSMC) and exhibited the most stable conditions and lowest temporal variability among the sampling sites. The comparatively smaller rise in groundwater level at LSMI, compared to LSMB and LSMC during the monitoring period suggests a weaker hydraulic response to surface water donation. This, together with the hydrochemical differences relative to LSMB and LSMC, indicates that LSMI is likely less connected to the surrounding groundwater system or is not located along the direct groundwater flow path between LSMB and LSMC. A plausible explanation could be local geological conditions that limit hydraulic connectivity. LSMI was characterized by the highest concentrations of Mg^{2+}, Na^{+}, and Cl^{-}, combined with low variability over time. This hydrochemical signature suggests longer groundwater residence times compared to LSMB and LSMC, as prolonged water-rock interaction leads to enrichment of major ions (Freeze & Cherry, 1979). Groundwater temperature and dissolved oxygen concentrations was lowest at LSMI among the three wells. These conditions represent the least favorable environment for microbial activity (Griebler & Mösslacher, 2003; Schwoerbel & Brendelberger, 2022), which is reflected by the lowest intracellular ATP and total cell count observed at this site. The low microbial activity likely explains the comparatively low CO_2 concentrations measured in LSMI (Aquilina et al., 2023). The lowest dissolved DIC concentrations among the wells observed at LSMI are likely linked to reduced CO_2 concentration. LSMI exhibited the highest concentrations of NH_4^{+}, phosphate (PO_4^{3-}), total phosphorus and iron (Fe^{2+}) among the three sampling sites. These elevated levels indicate stable and more reducing conditions compared to the other wells (Borch et al., 2010; Jiang et al., 2025b; McMahon & Chapelle, 2008). The gradual decline in sulfate concentrations over the monitoring period suggests progressive sulfate reduction and a further shift toward more reducing conditions. Only minor changes at LSMI can be attributed to surface water donation. An increase in groundwater temperature was observed during the donation phase, representing the only parameter that responded to the donation. In contrast, DOC concentrations decreased during the donation phase, which is the opposite effect observed at LSMB, indicating that surface water infiltration had little to no influence at this well. This interpretation is further supported by the contrasting DOC response at LSMB, where surface water donation caused an increase in DOC concentrations. Similarly, the slightly higher concentrations of soluble phosphorus and iron observed at LSMI during the donation period are unlikely to result directly from surface water input. These changes are more plausibly linked to temporarily increased reducing conditions that developed independently of the donation event.

4.6. Dynamics at LSMC

Groundwater level in LSMC showed the greatest variability among the three sampling sites. These fluctuations are probably influenced by pumping at the nearby drinking water production well. The groundwater level increase was the only measurable effect of surface water donation at this sampling site. LSMC was characterized by the highest dissolved oxygen concentrations and the strongest DO fluctuations among the three wells. This might be caused by the influence of pumping, as mixing induced by groundwater extraction likely introduces oxygen-rich water, while DO in groundwater can only enter from external sources such as surface water (Marmonier et al., 2023). The low ammonium concentrations at LSMC are also in connection with the higher oxygen availability at that site. Similarly, concentrations of phosphate, total phosphorus, sulfide and ferrous iron were also lowest in LSMC, suggesting less reducing conditions relative to the other wells. Intracellular ATP exhibited extremely high variability in groundwater from this well, likely reflecting the pronounced DO fluctuations. In this well vertical stratification of groundwater hydrochemistry was observed. DO concentrations were higher in the more shallow groundwater, while NH_4^+, PO_4^{3-}, total phosphorus, Fe^{2+} and Mn^{2+} were higher in the deeper groundwater. This indicates that the conditions were more reducing at the lower position. The observed stratification is likely influenced by the nearby pumping activity, which promotes mixing of the upper well water while leaving the lower layers more stable.

4.7. Fauna

LSMI, although showing chemically stable groundwater, exhibited the lowest groundwater temperature, the lowest dissolved oxygen (DO) concentrations, low microbial activity (reflected by low iATP, CO_2, and CH_4) and the lowest total cell counts (TCC) among the three wells. These conditions indicate an energetically and ecologically unfavorable environment. Oxygen is therefore considered a limiting factor for groundwater fauna, influencing both their abundance and vertical distribution within the aquifer (Hahn, 2006; Koch et al., 2021; Pospisil, 1994). Additionally, low food availability due to low productivity further limits groundwater fauna (Berkhoff, Bork & Hahn, 2015). The abundance of fauna was lowest at LSMI, often with zero or only one individual per sample . Also the proportion of stygobiont species was lowest at LSMI, while the proportion of stygoxene species, which occur accidently in groundwater (Marmonier et al., 2023), was highest, suggesting that low oxygen availability and limited biomass restrict the establishment of groundwater fauna. As mentioned before, LSMI showed the most reduced conditions among the three groundwater sampling sites. Negative correlation of absolute abundance of meiofauna with phosphate, total phosphorus and iron suggests that reduced conditions are less favorable for groundwater fauna. During donation phases fewer individuals were observed compared to periods without donation, highlighting the lack of a significant influence of donation at this well. In contrast, the shallow aquifer and groundwater at LSMB are strongly influenced by surface water donation. The infiltration of dissolved organic carbon (DOC) from surface water, combined with increased groundwater temperature, stimulates microbial biomass production. Microorganisms respond directly to the increased DOC availability, acting as the primary consumers of this energy source. Microbial communities and biofilms thus form one base of the groundwater food web, converting surface-derived organic matter into biomass that can be grazed by secondary consumers, mostly larger invertebrates. Consequently, periods of enhanced DOC input could possibly create temporarily favorable conditions for meiofauna, which respond to these short-term changes. This linkage between organic matter input, increased microbial biomass, and higher faunal diversity is consistent with previous findings (Marmonier et al., 2023). By contrast, low nutrient and oxygen availability limits both the abundance and diversity of hyporheic and stygophilic fauna (Schmidt, 2015). However, this effect is transient, and the well is unlikely to serve as a long-term habitat for meiofauna, as individual numbers decrease again after the donation period. During donation periods, absolute abundance increased significantly and showed positive correlations with temperature, DOC, microbial indicators (TCC and iATP), CH_4, and CO_2. These correlations highlight microbial biomass and energy availability as key drivers of the fauna response in LSMB. This pattern is consistent with findings by Datry et al. (2005), who demonstrated that groundwater recharge increases DOC availability and spatiotemporal heterogeneity, thereby enhancing invertebrate density and species richness, but in LSMB, the increase in species richness was observed only during the first 2023 donation phase, while absolute abundance increased in both donation periods. Cyclopoida were the dominant group across all groundwater sites, increasing over time at LSMB and particularly abundant during the 2024 donation. Oligochaeta, Amphipoda, Gastropoda and Isopoda, were present at the beginning of the monitoring period and during the first donation phase in 2023, but were largely absent afterward, indicate that LSMB is unlikely to support permanent populations of these taxonomic groups. LSMC exhibited the highest absolute abundance and greatest biodiversity among the three sites, including the largest number of different taxonomic groups. LSMC experiences continuous oxygenation events rather than episodic inputs like surface water donation. These conditions, together with sufficient microbial biomass and structural heterogeneity in the aquifer, create a more favorable habitat for meiofauna compared to the other two sites. Fauna data indicate that LSMC is largely unaffected by surface water donation, as many individuals were present prior to donation and population fluctuations occur independently of donation events. Seasonal trends, rather than donation events influence the pattern of the fauna abundance at LSMC.

4.8. Evaluation of the hypotheses

H1, predicting an increase in groundwater levels during surface water donation, was confirmed for all three sampling sites. LSMB, LSMI and LSMC showed significant groundwater level rises.

H2, suggesting an improvement in groundwater quality, was not confirmed. While parameters such as magnesium and electrical conductivity decreased at LSMB due to dilution, major ion and nutrient concentrations were already within drinking water standards before donation, indicating that the donation did not improve water quality. However the donation did also not impair the groundwater quality.

H3, the increase in dissolved organic carbon (DOC) during donation, was clearly observed at LSMB, reflecting surface water infiltration, whereas LSMI and LSMC showed no or opposite responses to the donation.

H4, proposing stimulated microbial activity during phases of surface water donation was strongly confirmed at LSMB, where total cell counts (TCC) and intracellular ATP (iATP) increased, but no significant changes were observed in the other two wells.

H5, predicting higher groundwater fauna abundance during donation, was partly supported for site LSMB. LSMI remained largely unaffected, while LSMC maintained high fauna abundance independent of donation.

Regarding H6, only LSMB, the well closest to the Fasangartenarm, exhibited pronounced responses to surface water donation, whereas LSMI (intermediate distance) and LSMC (most distant) remained largely unaffected.

5 Conclusion

Groundwater levels increased significantly at all three groundwater sampling sites during surface water donation periods, representing the only consistent common response across all sampling sites. Beyond this, measurable physical-chemical and biological changes were restricted to LSMB, the well closest to the surface water Fasangartenarm and most connected to it. The results demonstrate that in this case the impact of surface water donation is strongly site-specific, local and controlled by hydraulic connectivity to the surface water body. Surface water donation did not result in an impairment nor an improvement of groundwater quality. Groundwater temperature in this well increased during donation, reflecting the infiltration of warmer surface water during the summer period. Dissolved organic carbon concentrations increased significantly during donation, indicating the input of organic material from the surface. Microbial transport, growth and activity were stimulated by donation, reflected by the increase of total cell counts and intracellular ATP during donation. In addition nitrite and methane concentrations increased significantly, while sulfate concentrations decreased during donation, indicating intensified denitrification, sulfate reduction and methanogenesis. The surface water donation modifies redox reactions in LSMB, reflected by the reorganization of correlation structures among redox-sensitive parameters. Groundwater fauna abundance at LSMB also increased significantly during donation periods, suggesting temporary favorable habitat conditions. After the end of donation periods measured parameters largely returned to conditions prior to donation, indicating that the observed effects are transient rather than persistent. Overall, the findings demonstrate that surface water donation induces substantial short-term hydrochemical and ecological shifts, but these effects are spatially limited and strongly dependent on hydraulic connectivity.

The monitoring period included only two donation phases, limiting the ability to assess consistency across multiple cycles or to evaluate potential long-term effects. In addition, the study was based on three monitoring wells, which represents only a restricted area of the Upper Lobau and cannot fully represent the entire area. Future investigations should therefore include multiple donation cycles and extended monitoring periods to determine whether repeated donation events lead to long-term effects.

6 References

Alikhani, S., Nummi, P., & Ojala, A. (2021). *Urban wetlands: A review on ecological and cultural values*. *Water, 13*(22), 3301. https://doi.org/10.3390/w13223301.

Austrian Standards International. (1987). *ÖNORM ISO 7150-1: Wasseruntersuchung – Bestimmung von Ammonium – Manuelle spektrophotometrische Methode.* Austrian Standards.

Austrian Standards International. (2004). *ÖNORM EN ISO 6878: Wasserbeschaffenheit – Bestimmung von Phosphor – Photometrisches Verfahren mittels Ammoniummolybdat (ISO 6878:2004).* Austrian Standards International.

Appelo, C. A. J., & Postma, D. (2005). *Geochemistry, groundwater and pollution* (2nd ed.). A. A. Balkema Publishers.

Aquilina, L., Stumpp, C., Tonina, D., & Buffington, J. M. (2023). *Hydrodynamics and geomorphology of groundwater environments*. In F. Malard, C. Griebler & S. Rétaux (Eds.), *Groundwater ecology and evolution* (2nd ed., pp. 3–28). Academic Press.

Baart, I., Hohensinner, S., Zsuffa, I., & Hein, T. (2013). Supporting analysis of floodplain restoration options by historical analysis. *Environmental Science & Policy, 34,* 92–102. https://doi.org/10.1016/j.envsci.2012.10.003.

Barnett, D. J. M., Arts, I. C. W., & Penders, J. (2021). *microViz: An R package for microbiome data visualization and statistics*. *Journal of Open Source Software, 6*(63), 3201. https://doi.org/10.21105/joss.03201.

Becher, J., Griebler, C., Zosseder, K., & Bayer, P. (2025). Integrative assessment of urban groundwater quality in the city of Munich, Germany: Spatio-temporal patterns of hydrochemical and selected microbial indicators. *Journal of Hydrology, 658,* 133096. https://doi.org/10.1016/j.jhydrol.2025.133096.

Berkhoff, S. E., Bork, J., & Hahn, H. J. (2015). Die Metazoen-Fauna des Grundwassers. In H. Brendelberger, P. Martin, M. Brunke, & H. J. Hahn (Eds.), *Grundwassergeprägte Lebensräume* (pp. 25 - 30). E. Schweizerbart.

Berthold, F., Herick, K., & Siewe, R. M. (2000). Luminometer design and low light detection. *Methods in Enzymology, 305*, 62–87. https://doi.org/10.1016/S0076-6879(00)05478-1.

Borch, T., Kretzschmar, R., Kappler, A., Van Cappellen, P., Ginder-Vogel, M., Voegelin, A., & Campbell, K. (2010). Biogeochemical redox processes and their impact on contaminant dynamics. *Environmental Science & Technology, 44*(1), 15–23. https://doi.org/10.1021/es9026248.

Chapelle, F. H. (1993). *Ground-water microbiology and geochemistry*. Wiley.

Coder, L., Musolff, A., Kronsbein, P. M., Knöller, K., Büttner, O., Rinke, K., & Tittel, J. (2025). *How anthropogenic modification of riverscapes reduces the resilience of floodplain water bodies to drought*. *Ecological Engineering, 219*, 107686. https://doi.org/10.1016/j.ecoleng.2025.107686.

DIN Deutsches Institut für Normung. (1983). DIN 38406-1. *Deutsche Einheitsverfahren zur Wasser-, Abwasser- und Schlammuntersuchung; Kationen (Gruppe E); Bestimmung von Eisen (E 1).* DIN.

DIN Deutsches Institut für Normung. (1983). DIN 38406-2.*Deutsche Einheitsverfahren zur Wasser-, Abwasser- und Schlammuntersuchung; Kationen (Gruppe E); Bestimmung von Mangan (E 2).*DIN.

DIN Deutsches Institut für Normung. (1983). *DIN 38406-5: Deutsche Einheitsverfahren zur Wasser-, Abwasser- und Schlammuntersuchung; Kationen (Gruppe E); Bestimmung des Ammonium-Stickstoffs (E 5).* DIN.

DIN Deutsches Institut für Normung. (1990). *DIN 38405-21: Deutsche Einheitsverfahren zur Wasser-, Abwasser- und Schlammuntersuchung; Anionen (Gruppe D); Photometrische Bestimmung von gelöster Kieselsäure (D 21)*. DIN.

DIN Deutsches Institut für Normung. (1993). *DIN EN 26777: Wasserbeschaffenheit – Bestimmung von Nitrit – Spektrometrisches Verfahren (ISO 6777:1984); Deutsche Fassung EN 26777:1993*. DIN.

DIN Deutsches Institut für Normung. (1999). *DIN EN ISO 14911: Wasserbeschaffenheit – Bestimmung der gelösten Kationen Li^+, Na^+, NH_4^+, K^+, Mn^{2+}, Ca^{2+}, Mg^{2+}, Sr^{2+} und Ba^{2+} mittels Ionenchromatographie – Verfahren für Wasser und Abwasser (ISO 14911:1998); Deutsche Fassung EN ISO 14911:1999*. DIN.

DIN Deutsches Institut für Normung (2009). *DIN EN ISO 10304-1: Wasserbeschaffenheit – Bestimmung von gelösten Anionen mittels Flüssigkeits-Ionenchromatographie – Teil 1: Bestimmung von Bromid, Chlorid, Fluorid, Nitrat, Nitrit, Phosphat und Sulfat (ISO 10304-1:2007); Deutsche Fassung EN ISO 10304-1:2009*. DIN.

DIN Deutsches Institut für Normung (2017). *DIN 38405-27: Deutsche Einheitsverfahren zur Wasser-, Abwasser- und Schlammuntersuchung - Anionen (Gruppe D) - Teil 27: Bestimmung von Sulfid durch Gasextraktion (D 27)*. DIN.

Dunn, O. J. (1964). Multiple comparisons using rank sums. *Technometrics, 6*(3), 241–252. https://doi.org/10.1080/00401706.1964.10490181.

Epting, J., Råman Vinnå, L., Piccolroaz, S., Affolter, A., & Scheidler, S. (2022). Impacts of climate change on Swiss alluvial aquifers – A quanitative forecast focused on natural and artificial groundwater recharge by surface water infiltration. Journal of Hydrology X, 17. https://doi.org/10.1016/j.hydroa.2022.100140.

Faulkner, S. (2004). Urbanization impacts on the structure and function of forested wetlands. *Urban ecosystems*, *7*(2), 89-106.

Feng, F., Jiang, Y., Jia, Y., Shang, C., Lian, X., Zang, Y., & Zhao, M. (2023). Risks of nutrients and metal(loid)s mobilization triggered by groundwater recharge containing reactive organic matter. *Journal of Hydrology, 623*, 129780. https://doi.org/10.1016/j.jhydrol.2023.129780.

Fillinger, L., Hug, K., & Griebler, C. (2021). Aquifer recharge viewed through the lens of microbial community ecology: Initial disturbance response, and impacts of species sorting versus mass effects on microbial community assembly in groundwater during riverbank filtration. *Water Research, 189*, 116631. https://doi.org/10.1016/j.watres.2020.116631.

Fox, J., & Weisberg, S. (2019). *An R companion to applied regression* (3rd ed.). Sage. https://www.john-fox.ca/Companion/.

Freeze, R. A., & Cherry, J. A. (1979). *Groundwater*. Prentice-Hall.

Funk, A., Reckendorfer, W., Kucera-Hirzinger, V., Raab, R., & Schiemer, F. (2009). Aquatic diversity in a former floodplain: Remediation in an urban context. *Ecological Engineering, 35*(10), 1476–1484. https://doi.org/10.1016/j.ecoleng.2009.06.013.

Gaviria-Melo, S., & Fuchs, A. (2020). Bestimmung von Evertebraten des Grundwassers. Universität Wien, Wien.

Goodsell, D. S. (1996). Our Molecular Nature. Springer, New York, USA.

Gosset, W. S. (1908). The probable error of a mean. *Biometrika, 6*(1), 1–25. https://doi.org/10.2307/2331554.

Griebler, C. & Mösslacher, F. (2003). Grundwasser-Ökologie. Facultas.

Habellöcker, S. (2023). *Ecological monitoring of the surface water donation to the Upper Lobau with a focus on physical-chemical conditions* (Unpublished Bachelor's thesis). University of Vienna, Vienna, Austria.

Havril, T., Tóth, Á., Molson, J. W., Galsa, A., & Mádl-Szőnyi, J. (2018). Impacts of predicted climate change on groundwater flow systems: Can wetlands disappear due to recharge reduction? *Journal of Hydrology, 563*, 1169–1180. https://doi.org/10.1016/j.jhydrol.2017.09.020.

Hein, T., Blaschke, A. P., Haidvogl, G., Hohensinner, S., Kucera-Hirzinger, V., Preiner, S., Reiter, K., Schuh, B., Weigelhofer, G., & Zsuffa, I. (2006). Optimised management strategies for the Biosphere reserve Lobau, Austria – Based on a multi-criteria decision support system. *Ecohydrology and Hydrobiology, 6*(1–4), 25–36. https://doi.org/10.1016/S1642-3593(06)70123-9.

Hupach, S., & Bayerl, A. (2018). Der Kohlenstoffgehalt im Reinstwasser. Nachrichten Aus Der Chemie, 66(5), 528–529. https://doi.org/10.1002/nadc.20184075594.

Jäger, A., & Hahn, H. J. (2022). Techniques for sampling and monitoring of groundwater fauna. In T. Mehner & T. Trockner (Eds.), *Encyclopedia of Inland Waters* (2nd ed., Vol. 3, pp. 600–610). Elsevier. https://doi.org/10.1016/B978-0-12-819166-8.00193-6.

Ji, H., Chang, W., Cai, L., Wang, N., Li, C., & Huang, K. (2025). Geochemical and hydrological processes control the distribution of high iron and manganese concentrations in groundwater within Quaternary aquifers. *Journal of Hydrology, 663*(Part A), 134063. https://doi.org/10.1016/j.jhydrol.2025.134063.

Jiang, T., Sun, T., Guo, Z., Lu, J., Liu, F., & Guan, X. (2025a). Effects of ecological water replenishment on microbial denitrification in aquatic environment of infiltration area. *Journal of Hazardous Materials, 494,* 138688. https://doi.org/10.1016/j.jhazmat.2025.138688.

Jiang, J., Su, C., Geng, H., Wang, Y., Ge, W., Pan, H., Xie, X., & Feng, G. (2025b). *Fe and Mn biogeochemical cycling associated with basin-scale redox dynamics traced by DOM degradation in different alluvial aquifers*. *Water Research, 282*, 123759. https://doi.org/10.1016/j.watres.2025.123759.

Jin, Z., Meng, X., Tang, S., Shen, Z., Yuan, L., Chen, L., Xu, Z., Chen, D., & Liu, Z. (2024). Areal artificial recharge has changed the interactions between surface water and groundwater. *Journal of Hydrology, 637*, 131318. https://doi.org/10.1016/j.jhydrol.2024.131318.

Kölle, W. (2017). Anorganische Wasserinhaltsstoffe, Hauptkomponenten. In Wasseranalysen – richtig beurteilt, W. Kölle (Ed.). https://doi.org/10.1002/9783527807871.ch4.

Kruskal, W. H., & Wallis, W. A. (1952). Use of ranks in one-criterion variance analysis. *Journal of the American Statistical Association, 47*(260), 583–621. https://doi.org/10.1080/01621459.1952.10483441.

Kundu, S., Kundu, B., Rana, N. K., & Mahato, S. (2024). *Wetland degradation and its impacts on livelihoods and sustainable development goals: An overview*. *Sustainable Cities and Society*. Advance online publication. https://doi.org/10.1016/j.spc.2024.05.024.

Lee, J.-H., & Lee, B.-J. (2018). *Microbial reduction of Fe(III) and SO_4^{2-} and associated microbial communities in the alluvial aquifer groundwater and sediments*. Microbial Ecology, 76(1), 182–191. https://doi.org/10.1007/s00248-017-1119-3.

Levene, H. (1960). *Robust tests for equality of variances.* In I. Olkin (Ed.), *Contributions to probability and statistics: Essays in honor of Harold Hotelling* (pp. 278–292). Stanford University Press.

Li, N., Lyu, H., Xu, G., Chi, G., & Su, X. (2023). Hydrogeochemical changes during artificial groundwater well recharge. *Science of the Total Environment, 900,* 165778. https://doi.org/10.1016/j.scitotenv.2023.165778.

Li, Q., Chen, X., Zhang, W., Wu, F., & Zhang, Y. (2026). *Transport of bacterial cell and spore from different recharge water resources in porous media during simulated artificial groundwater recharge*. Colloids and Surfaces B: Biointerfaces, 258, 115290. https://doi.org/10.1016/j.colsurfb.2025.115290.

Liu, C., Li, X., Mansoldo, F. R. P., An, J., Kou, Y., Zhang, X., Zeng, J., Vermelho, A. B., & Yao, M. (2022). Microbial habitat specificity largely affects microbial co-occurrence patterns and functional profiles in wetland soils. *Geoderma, 418,* 115866. https://doi.org/10.1016/j.geoderma.2022.115866.

López Lloreda, C., Maze, J., Wardinski, K., Corline, N., McLaughlin, D., Jones, C. N., Scott, D., Palmer, M., & Hotchkiss, E. R. (2024). CO_2 and CH_4 concentrations in headwater wetlands influenced by morphology and changing hydro-biogeochemical conditions. *Ecosystems, 27*(5), 999–1019. https://doi.org/10.1007/s10021-024-00936-7.

Mackereth, F. J. H., Heron, J., & Talling, J. F. (1989). Water analysis: Some revised methods for limnologists (2. impr). Freshwater Biological Association. 13-14.

Marmonier, P., Galassi, D. M. P., Korbel, K., Close, M., Datry, T., & Karwautz, C. (2023). *Groundwater biodiversity and constraints to biological distribution*. In F. Malard, C. Griebler & S. Rétaux (Eds.), *Groundwater ecology and evolution* (2nd ed., pp. 113–140). Academic Press.

McMahon, P. B., & Chapelle, F. H. (2008). Redox Processes and Water Quality of Selected Principal Aquifer Systems. *Ground Water*, *46*(2), 259–271. https://doi.org/10.1111/j.1745-6584.2007.00385.x.

McMurdie, P. J., & Holmes, S. (2013). *phyloseq: An R package for reproducible interactive analysis and graphics of microbiome census data*. *PLoS ONE, 8*(4), e61217. http://dx.plos.org/10.1371/journal.pone.0061217.

Mitsch, W. J. (2005). Wetland creation, restoration, and conservation: A Wetland Invitational at the Olentangy River Wetland Research Park. *Ecological Engineering*, *24*(4), 243–251. https://doi.org/10.1016/j.ecoleng.2005.02.006.

Ogle, D. H., Doll, J. C., Wheeler, A. P., & Dinno, A. (2025). *FSA: Simple fisheries stock assessment methods* (R package version 0.9.6). https://CRAN.R-project.org/package=FSA.

Opperman, J. J., Galloway, G. E., Duvail, S., Chivava, F., & Johnson, K. A. (2024). *River-floodplain connectivity as a nature-based solution to provide multiple benefits for people and biodiversity.* In S. M. Scheiner (Ed.), *Encyclopedia of biodiversity* (3rd ed., pp. 620–645). Academic Press. https://doi.org/10.1016/B978-0-12-822562-2.00047-5

Parlov, J., Kovač, Z., Nakić, Z., & Barešić, J. (2019). Using water stable isotopes for identifying groundwater recharge sources of the unconfined alluvial Zagreb aquifer (Croatia). *Water, 11*(10), 2177. https://doi.org/10.3390/w11102177.

Pedersen, T. L. (2024). *patchwork: The composer of plots* (R package version 1.3.0). https://CRAN.R-project.org/package=patchwork.

Potter, B. B., & Wimsatt, J. C. (2012). USEPA method 415.3: Quantifying TOC, DOC, and SUVA. Journal - American Water Works Association, 104(6), E358–E369. https://doi.org/10.5942/jawwa.2012.104.0086.

Preiner, S., Weigelhofer, G., Funk, A., Hohensinner, S., Reckendorfer, W., Schiemer, F., & Hein, T. (2018). Danube floodplain Lobau. In S. Schmutz & J. Sendzimir (Eds.), *Riverine ecosystem management: Science for governing towards a sustainable future* (pp. 491–506). Springer. https://doi.org/10.1007/978-3-319-73250-3_25.

R Core Team (2024). _R: A Language and Environment for Statistical Computing_. R Foundation for Statistical Computing, Vienna, Austria. <https://www.R-project.org/>.

Riedel, T. (2019). Temperature-associated changes in groundwater quality. *Journal of Hydrology, 572,* 206–212. https://doi.org/10.1016/j.jhydrol.2019.02.059

Rieseberg, M., Kasper, C., Reardon, K. F., & Scheper, T. (2001). Flow cytometry in biotechnology. *Applied Microbiology and Biotechnology, 56*(3–4), 350–360. https://doi.org/10.1007/s002530100673.

Rivett, M. O., Buss, S. R., Morgan, P., Smith, J. W. N., & Bemment, C. D. (2008). Nitrate attenuation in groundwater: A review of biogeochemical controlling processes. *Water Research, 42*(16), 4215–4232. https://doi.org/10.1016/j.watres.2008.07.020.

Schmidt, S. I. (2015). Abiotik und Stoffumsätze. In H. Brendelberger, P. Martin, M. Brunke, & H. J. Hahn (Eds.), *Grundwassergeprägte Lebensräume* (pp. 15-19). E. Schweizerbart.

Schwoerbel, J., & Brendelberger, H. (2022). *Einführung in die Limnologie: Stoffhaushalt – Lebensgemeinschaften – Technologie* (11. Aufl.). Springer Spektrum. https://doi.org/10.1007/978-3-662-63334-2.

Shapiro, S.S. and Wilk, M.B., 1965. An analysis of variance test for normality (complete samples). *Biometrika*, 52(3–4), pp.591–611. https://doi.org/10.1093/biomet/52.3-4.591.

Spearman, C. (1904). *The proof and measurement of association between two things.* American Journal of Psychology, 15, 72–101. https://doi.org/10.2307/1412159.

Tena, A., Piégay, H., Seignemartin, G., Barra, A., Berger, J. F., Mourier, B., & Winiarski, T. (2020). *Cumulative effects of channel correction and regulation on floodplain terrestrialisation patterns and connectivity*. *Geomorphology, 354*, Article 107034.https://doi.org/10.1016/j.geomorph.2020.107034.

Teresa, M., Piedade F., Wittmann, F., Schöngart, J., Junk, W. J., & Parolin, P. (2024). Wetlands ecosystems. In S. A. Levin (Ed.), *Encyclopedia of biodiversity* (3rd ed., Vol. 1, pp. 581–599). Elsevier. https://doi.org/10.1016/B978-0-12-822562-2.00158-4.

Veal, D. A., Deere, D., Ferrari, B., Piper, J., & Attfield, P. V. (2000). Fluorescence staining and flow cytometry for monitoring microbial cells. *Journal of Immunological Methods, 243*(1–2), 191–210. https://doi.org/10.1016/s0022-1759(00)00234-9.

Wang, J., Niu, Y., Li, C., Liu, Z., Jiang, X., & Wu, Y. (2025). Surface water and groundwater interactions contributed the seasonal NO_3^- and NH_4^+ sources and transformations in a hilly region, China. *Journal of Environmental Management, 387,* 125750. https://doi.org/10.1016/j.jenvman.2025.125750.

Wang, X., Xu, H., Waheed, A., Liu, K., Zhao, X., & Zhang, Q. (2026). Hydrological connectivity drives groundwater fluctuations and water quality dynamics in the Taitema Lake wetland ecosystem. *Journal of Arid Environments, 232,* 105524. https://doi.org/10.1016/j.jaridenv.2025.105524.

Wei, T., & Simko, V. (2024). *R package 'corrplot': Visualization of a correlation matrix* (Version 0.95) [R package]. https://github.com/taiyun/corrplot.

Weigelhofer, G., Janac, P., & Hein, T. (2005). Erkenntnisse zur Ökologie aus dem Wasserwirtschaftlichen Versuch „Dotation Obere Lobau, Wien" für eine nachhaltige Entwicklung urbaner Augewässer. *Österreichische Wasser- und Abfallwirtschaft*, *57*(9–10), a16–a19. https://doi.org/10.1007/BF03164452.

Weigelhofer, G., Hein, T., Kucera-Hirzinger, V., Zornig, H., & Schiemer, F. (2011). Hydrological improvement of a former floodplain in an urban area: Potential and limits. *Ecological Engineering, 37*(10), 1507–1514. https://doi.org/10.1016/j.ecoleng.2011.05.005.

Weigelhofer, G., Reckendorfer, W., Funk, A., & Hein, T. (2013). Auenrevitalisierung – Potenzial und Grenzen am Beispiel der Lobau, Nationalpark Donau-Auen. *Österreichische Wasser- und Abfallwirtschaft*, *65*(11–12 S.400–407), 400–407. https://doi.org/10.1007/s00506-013-0115-1.

Whalen, P. A., Tracey, D. R., & Duguay, J. (2018). Adenosine Triphosphate (ATP) measurement technology. Microbial Sensors for Drinking Water Industry, 137-154.

Wickham, H. (2016). *ggplot2: Elegant graphics for data analysis*. Springer-Verlag, New York. https://ggplot2.tidyverse.org.

Wickham, H., Averick, M., Bryan, J., Chang, W., McGowan, L. D., François, R., Grolemund, G., Hayes, A., Henry, L., Hester, J., Kuhn, M., Pedersen, T. L., Miller, E., Bache, S. M., Müller, K., Ooms, J., Robinson, D., Seidel, D. P., Spinu, V., Takahashi, K., Vaughan, D., Wilke, C., Woo, K., & Yutani, H. (2019). *Welcome to the tidyverse*. *Journal of Open Source Software, 4*(43), 1686. https://doi.org/10.21105/joss.01686.

Wilcoxon, F. (1945). Individual comparisons by ranking methods. *Biometrics Bulletin, 1*(6), 80–83. https://doi.org/10.2307/3001968.

Wittmann, F. (2022). The landscape role of river wetlands. In *Encyclopedia of Inland Waters* (2nd ed., Vol. 3, pp. 51-64). Elsevier. https://doi.org/10.1016/B978-0-12-819166-8.00191-2.

Xie, Y. (2024). *knitr: A general-purpose package for dynamic report generation in R* (R package version 1.49). https://yihui.org/knitr/.

Ye, P., Hao, X., & Cao, Y. (2018). *Analysis on ecological protection of urban wetland. Natural Resources Conservation and Research, 1*(1). https://doi.org/10.24294/nrcr.v1i1.226.

Yin, G., Xu, X., Li, T., Wang, T., Haw Yen, H., Hua, L., Jiao, H., Tong, B., Du, X., Wen, H., & Li, W. (2025). *Interactions between soil water and groundwater differ during artificial recharge and extreme rainfall periods*. Agricultural Water Management, 321, 109944. https://doi.org/10.1016/j.agwat.2025.109944.

6.1. Internet sources

IS1: Stadt Wien (n.d. a). Lobau – Wiens Beitrag zum Nationalpark, retrieved September 23rd, 2025, Lobau - Wiens Beitrag zum Nationalpark - Stadt Wien.

IS2: Stadt Wien (n.d. b). Künstliche Wasserzufuhr gegen Austrocknung der Oberen Lobau, retrieved September 23rd, 2025, Künstliche Wasserzufuhr gegen Austrocknung der Oberen Lobau - Stadt Wien.

IS3: Stadt Wien (n.d. c). Neue Dotation schützt Obere Lobau, retrieved September 23rd, 2025, Neue Dotation schützt Obere Lobau - Stadt Wien.

IS4: Geosphere Austria (2025). Messstationen Tagesdaten v2, Niederschlag 24h Summe, March 1st 2023 – January 23rd 2025, Messstation Groß-Enzersdorf 5972, retrieved November 3rd, 2025, GeoSphere Austria Data Hub.

IS 5: Republik Österreich. (2001). *Trinkwasserverordnung (TWV), BGBl. II Nr. 304/2001 (konsolidierte Fassung vom 27. Dezember 2025).* Rechtsinformationssystem des Bundes (RIS). Retrieved December 27, 2025, RIS - Trinkwasserverordnung - Bundesrecht konsolidiert, Fassung vom 27.12.2025.

IS 6: *Trinkwasserbefund* (2025). Retrieved December 27th, 2025, Trinkwasserbefund.

7 List of Figures

Figure 1. Locations of the monitoring groundwater wells LSMB, LSMI and LSMC, production well Markethäufel (PW), Panozzalacke and Fasangartenarm (FA) (base map: Google Maps; modified by the author). The area between the red dashed lines indicates the zone where surface water is present during donation periods. The pipeline (in red) marks the route through which water flows from the New Danube into the Panozzalacke. 6

Figure 2 Groundwater levels at LSMB, LSMI, and LSMC (meters above sea level, m a.s.l.). Filled points indicate donation periods. 14

Figure 3. Groundwater levels (m a.s.l.) in the wells LSMB, LSMI, and LSMC during donation (left) and no-donation (right) periods. 15

Figure 4. Dissolved oxygen (mg/L) in gw over time at the three monitoring wells showing measurements at both well positions (up and down). Filled squares indicate surface water donation periods. 16

Figure 5. Boxplots of a) electrical conductivity (EC), b) dissolved oxygen (DO, logarithmic scale), c) temperature, and d) pH. The box of Panozzalacke is based on all samples collected across the entire monitoring period. In the ‚Donation' plot the surface water Fasangartenarm (Fasan) is included, which only contained surface water during donation periods. 18

Figure 6. Boxplots of a) calcium (Ca^{2+}), b) magnesium (Mg^{2+}). The box of Panozzalacke (Panozza) is based on all samples collected across the entire monitoring period. In the ‚Donation' plot the surface water Fasangartenarm (Fasan) is included, which only contained surface water during donation periods. 20

Figure 7 a) Sodium (Na^{+}) and b) potassium (K^{+}) over time at the three groundwater wells showing measurements at both well positions (up and down). Filled squares indicate surface water donation. 20

Figure 8 a) Ammonium (NH_4^{+}), b) Phosphate (PO_4^{3-}) and c) total phosphorus (P total) over time at the three groundwater wells showing measurements at both well positions (up and down). Filled squares indicate surface water donation periods. 23

Figure 9. a) Nitrate (NO_3^{-}) and b) nitrite (NO_2^{-}) over time at the three groundwater wells showing measurements at both well positions (up and down). Filled squares indicate surface water donation periods. 25

Figure 10 Boxplots of Sulfate (SO_4^{2-}) The box of Panozzalacke (Panozza) is based on all samples collected across the entire monitoring period. In the ‚Donation' plot the surface water Fasangartenarm (Fasan) is included, which only contained surface water during donation periods. 26

Figure 11 a) Sulfate (SO_4^{2-}) and b) sulfide (HS^{-}) over time at the three groundwater wells showing measurements at both well positions (up and down). Filled squares indicate surface water donation periods. 27

Figure 12 a) Iron (Fe^{2+}; µg/L) and b) manganese (Mn^{2+}; µg/L) over time at the three groundwater wells showing measurements at both well positions (up and down). Filled squares indicate periods of donation. 28

Figure 13. Boxplots of a) dissolved organic carbon (DOC) and b) dissolved inorganic carbon (DIC). The box of Panozzalacke (Panozza) is based on all samples collected across the entire monitoring period. In the ‚Donation' plot the surface water Fasangartenarm (Fasan) is included, which only contained surface water during donation periods. 30

Figure 14. Boxplots of a) total cell counts (TCC) and b) intracellular ATP. The box of Panozzalacke (Panozza) is based on all samples collected across the entire monitoring period. In the ‚Donation' plot the surface water Fasangartenarm (Fasan) is included, which only contained surface water during donation periods. The y-axis of both plots is displayed in a logarithmic scale. 32

Figure 15. a) Methane (CH_4) and b) carbon dioxide(CO_2) over time at the three groundwater wells showing measurements at both well positions (up and down). Filled points and grey background indicate periods of donation. 34

Figure 16. Boxplots of a) methane (CH_4) and b) carbon dioxide (CO_2). The box of Panozzalacke (Panozza) is based on all samples collected across the entire monitoring period. In the ‚Donation' plot the surface water Fasangartenarm (Fasan) is included, which only contained surface water during donation periods. 34

Figure 17 Proportional occurrence of stygobiont, stygophile, and stygoxene taxonomic groups, based on all individuals collected during the monitoring period. 35

Figure 18. Absolute abundance and taxonomic composition of groundwater fauna at the sampling sites LSMB, LSMI and LSMC across the entire sampling period. Each bar represents one sampling event. Grey backgrounds indicate donation periods. 38

Figure 19. Pie charts showing the relative abundances of the recorded taxonomic groups at the three groundwater sampling sites LSMB, LSMI, and LSMC. For each sampling site, proportions are based on all individuals collected over the entire monitoring period. 40

Figure 20. Relative abundance (%) of LSMB, LSMI, and LSMC, separated by donation and non-donation periods. 42

Figure 21. Shannon diversity at the three groundwater sampling sites (LSMB, LSMI, LSMC) during donation and non-donation periods. 43

Figure 22. Species richness at the three groundwater sampling sites (LSMB, LSMI, LSMC) during donation and non-donation phases. 44

Figure 23. Spearman correlation matrices of measured and analysed parameters during donation and during periods without surface water donation. The matrices show a) LSMB during donation, b) LSMB without donation, c) LSMI and LSMC during donation and d) LSMI and LSMC without donation. Color intensity represents Spearman's rank correlation coefficients (ρ), with blue indicating positive correlations and red indicating negative correlations. 47

8 List of Tables

Table 1. Coordinates of sampling sites and well depths for groundwater wells........................ 6

Table 2. Sampling dates during donation and no donation periods. 12

Table 3. Number of individuals recorded for each taxonomic group at the three groundwater monitoring sites, shown separately for donation and non-donation periods. 37

Table 4. Statistical comparison of ion concentrations between surface water donation and periods without water supply.. 70

9 Appendix

parameter	sampling site	Result of paired t-test or Wilcoxon signed-rank test
Ca^{+} (mg/L)	LSMB	W = 158, p = 0.144
Ca^{+} (mg/L)	LSMI	W = 247.5, p = 0.431
Ca^{+} (mg/L)	LSMC	W = 240.5, p = 0.542
Mg^{2+} (mg/L)	LSMB	t = -4.243, df = 40, p = 1.27
Mg^{2+} (mg/L)	LSMI	W = 199, p = 0.674
Mg^{2+} (mg/L)	LSMC	W = 228, p = 0.769
K (mg/L)	LSMB	t = 0.51, df = 40, p = 0.612
K (mg/L)	LSMI	W = 263.5, p = 0.226
K (mg/L)	LSMC	W = 270.5, p = 0.164
Na^{+} (mg/L)	LSMB	t = -4.695, df = 40, p = 0.379
Na^{+} (mg/L)	LSMI	W = 201, p = 0.712
Na^{+} (mg/L)	LSMC	W = 212.5, p = 0.939
Cl^{-} (mg/L)	LSMB	W = 165, p = 0.199
Cl^{-} (mg/L)	LSMI	t = 0.738, df = 40, p = 0.465
Cl^{-} (mg/L)	LSMC	W = 229.5, p = 0.741
SiO_4 (mg/L)	LSMB	W = 266.5, p = 0.203
SiO_4 (mg/L)	LSMI	t = -0.029, df = 40, p = 0.977
SiO_4 (mg/L)	LSMC	W = 172, p = 0.267

Table 4. Statistical comparison of ion concentrations between surface water donation and periods without water supply.